Live from

Science that saves the world - *from* forefront science *to* more resilient societies.

A prosperous, happy inter-seismic period.

It's the year 2025 in northwest Washington state, USA. Residents and tourists enjoy majestic mountains, pristine coastlines, and efficient clean energy and transportation. Commerce thrives on robust telecommunications and transportation. Land-use planners, policy-makers and business owners have located infrastructure away from areas most vulnerable to earthquake hazards, and invested wisely in hazard-mitigating measures where most effective.

USGS science for a changing world

Resilience-building products, underlain by science.

building codes & designs

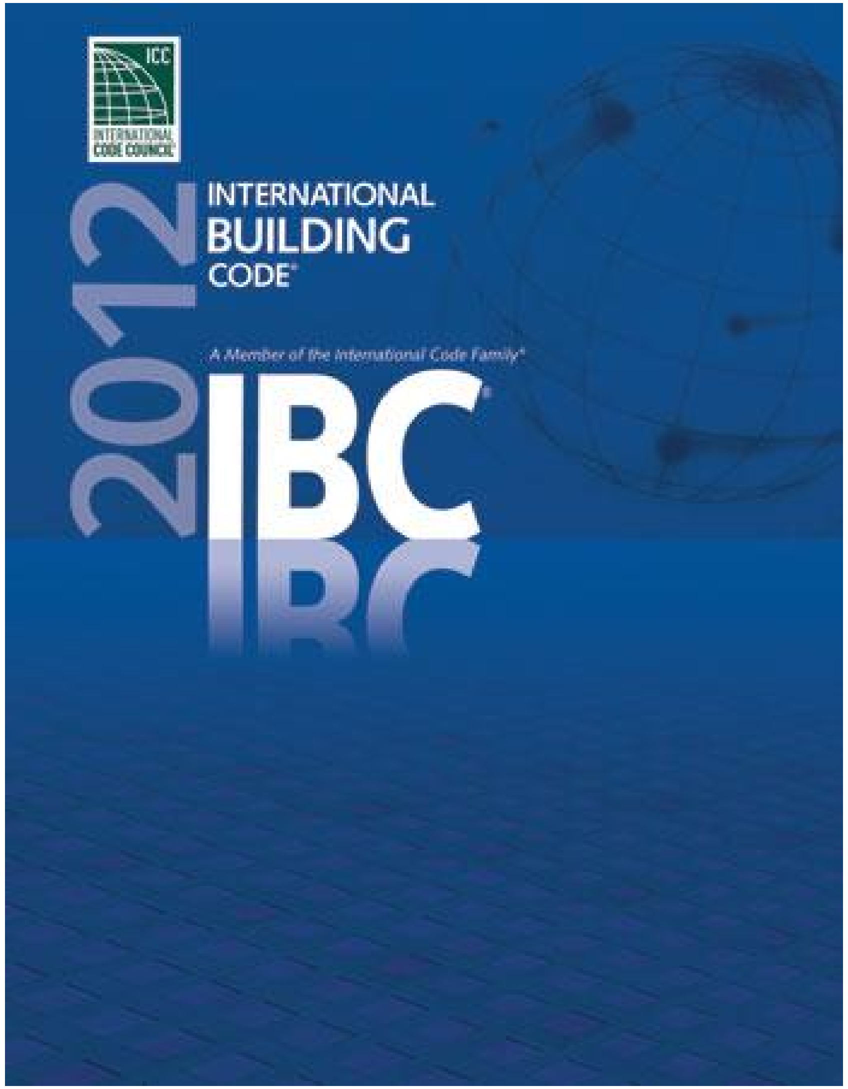

impact forecasts

1-Year Natural and Induced Earthquake Damage Forecast

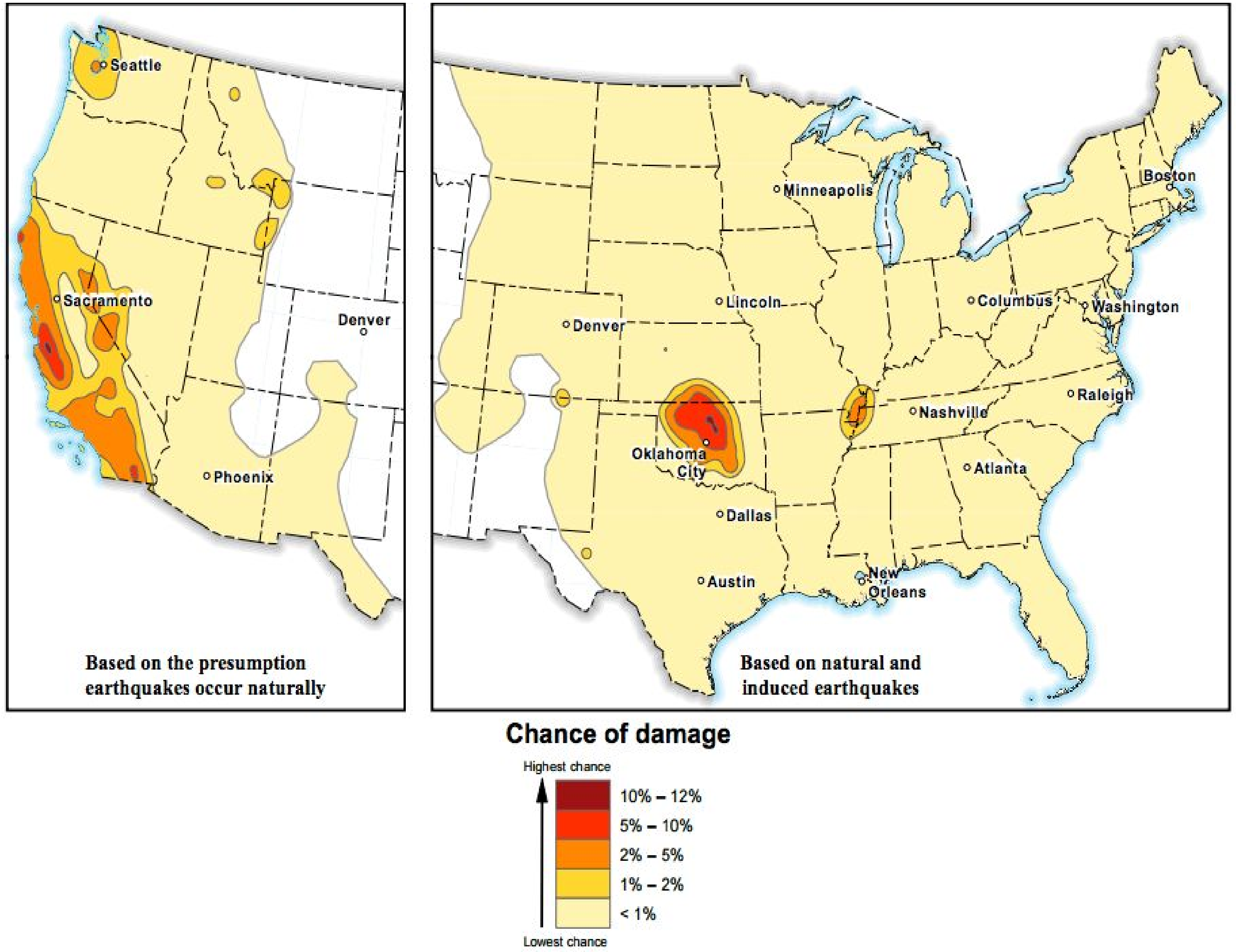

CASCADIA
RISING

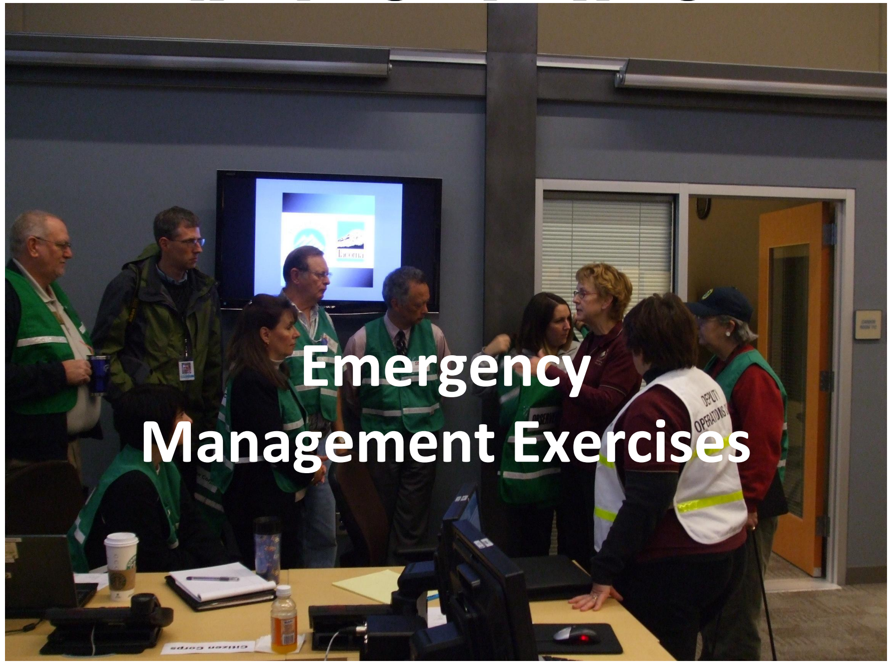

educational materials

Educational Scenarios

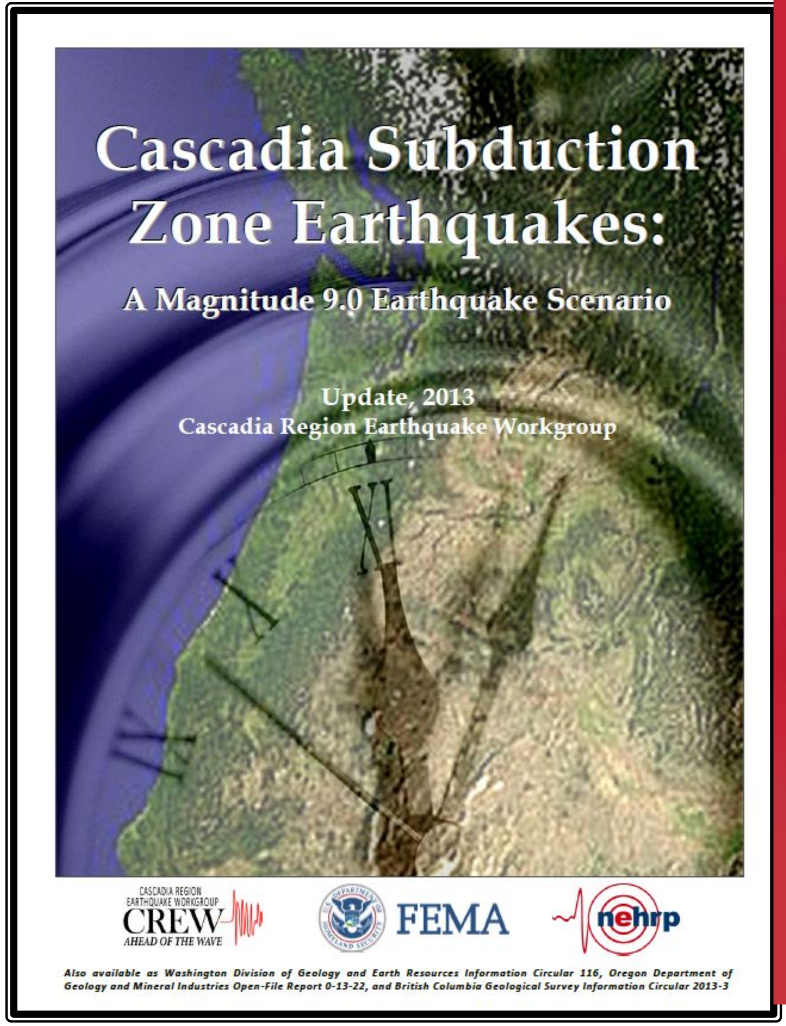

Non-fiction Literature

THE REALLY BIG ONE

(New Yorker, 7/20/15)

Hollywood

Forefront science provides the long-term context.

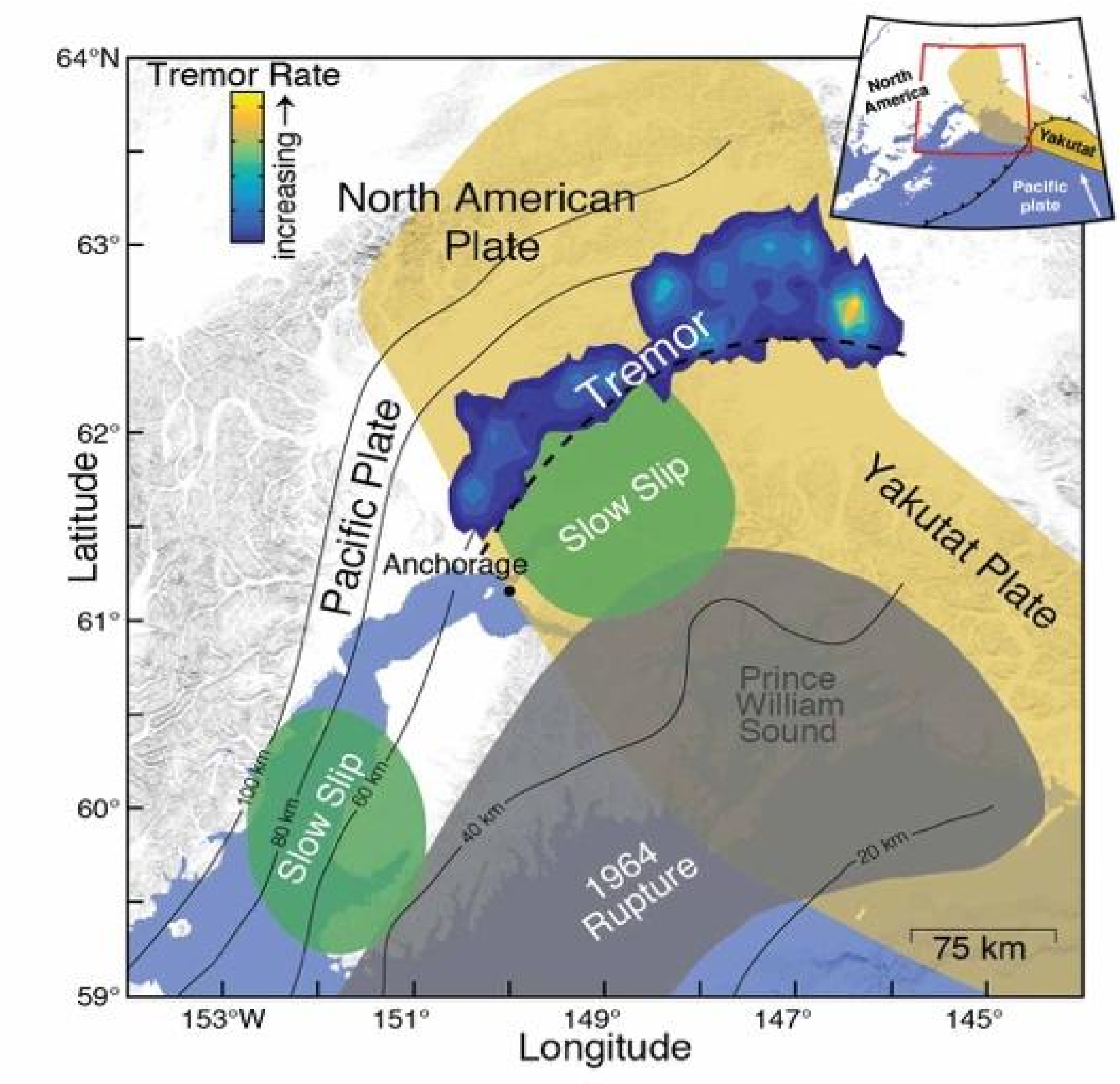

multi-disciplinary studies define slipping surfaces (where & how).

newly defined tremor distribution in central Alaska indicates the Yakutat plate actively slips over the North American plate (in addition/instead of the Pacific plate).

Wech, 2016.

robust recurrence estimates require multiple observation types

The onshore tsunami & coastal uplift/subsidence record

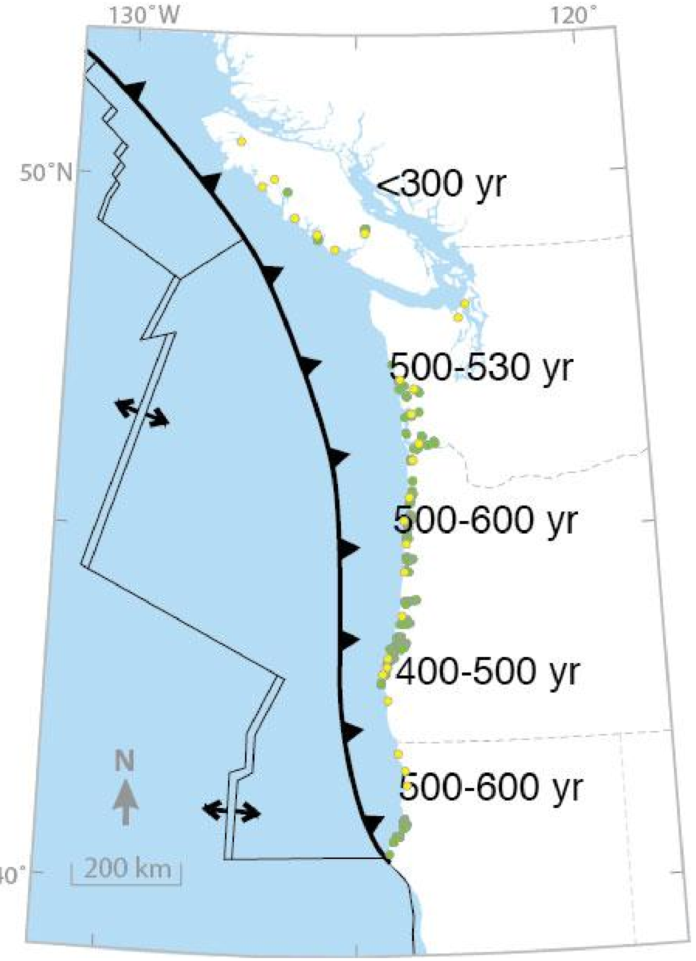

The offshore turbidite & sediment record

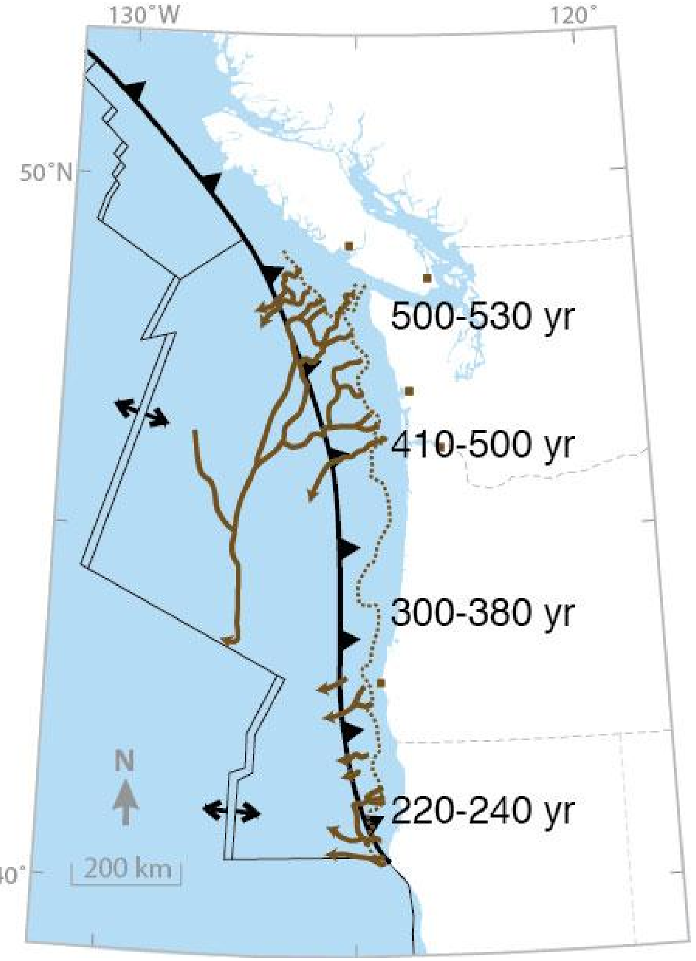

limited earthquake observations necessitate cycle models built on sound theory

Table 1. Summary of Equations[a]

Equation	Meaning
Viscoplastic material response	
$\dot{\epsilon}_{eq} = \sqrt{\frac{2}{3}\dot{\epsilon}_{ij}\dot{\epsilon}_{ij}}$	equivalent strain rate—equation (54)
$\sigma_{eq} = \sqrt{\frac{3}{2}s_{ij}s_{ij}}$	equivalent stress—equation (55)
$\sigma_{eq} = \sigma_0 \left[1 + \beta_0 \log\left(\frac{\dot{\epsilon}_{eq}}{\dot{\epsilon}_0}\right)\right]$	nonlinear viscous response—equation (56)
σ_0, β_0, and $\dot{\epsilon}_0$	positive material constants
$t_0 = \frac{1}{\dot{\epsilon}_0} \exp\left(\frac{1}{\beta_0}\right)$	characteristic viscoplastic time—equation (59)
$\sigma_\Omega = \sigma_0 \beta_0$	characteristic resistance stress—equation (60)
Macroscopic quantities	
V	sliding velocity
W	normal force
F	friction (shear) force
$\sigma = \frac{W}{\Sigma_0}$	nominal normal stress
$\tau = \frac{F}{\Sigma_0}$	nominal shear stress
$\mu = \frac{\tau}{\sigma}$	macroscopic friction coefficient
Σ_0	nominal (apparent) contact surface
$\Sigma_r = \Sigma_r^e + \Sigma_r^p$	real contact surface—equation (12)
Σ_r^e	total area of elastic contacts
Σ_r^p	total area of plastic contacts
$\Sigma_{r(ss)}^p = \frac{\sigma}{\sigma_*}\Sigma_r^{p*}\left[1 - \beta_\Sigma \log\left(\frac{V}{V_*}\right)\right]$	velocity and stress dependence of
	the plastic contact area at steady state—equation (31)
$\mu(V,\theta) = \mu_* + a\log\left(\frac{V}{V_*}\right) + b\log\left(\frac{\theta}{\theta_*}\right)$	phenomenological friction law—equation (2)
θ	state variable
μ_*, V_*, θ_*	reference values of friction, sliding velocity
	and state parameter
$\dot{\theta}_1$	growth rate of the state variable
	during static contact
$\hat{c}_V = 1 - \dot{\theta}_1$	parameter characterizing the velocity dependence
	of the evolution law—equation (105)
$d_c = V_*\theta_*$	characteristic length scale
	for the evolution of friction—equation (38)
$\dot{\theta} = \hat{F}(\theta, V) - \frac{a}{b}\hat{c}_V\theta\frac{\dot{V}}{V} - \frac{\hat{c}_\sigma\theta}{b\sigma}\dot{\sigma}$	modified evolution law—equation (8)
$\hat{F}(\theta, V) = (1 - \hat{c}_V)F(\theta, V)$	modified aging law—equation (9)
N	total number of contacts
Elastic contacts	
N_e	number of elastic contacts
$f_e = \frac{N_e}{N}$	proportion of elastic contacts—equation (10b)
W_e	resultant of the normal forces carried by elastic contacts
$w_e = \frac{W_e}{N_e}$	normal force at an individual elastic contact—equation (14a)
F_e	resultant of the tangential forces carried by elastic contacts
$\mu_e = \frac{F_e}{W_e}$	friction coefficient of elastic contacts
Plastic contacts	
h_*	reference height of the plastic cylindrical contacts
$\frac{N_p}{N} = 1 - f_e$	proportion of plastic contacts—equation (10c)

"We present a micromechanical model for rate and state friction in which the contact between the two surfaces occur via plastic and elastic contacts…
we identify the state variable as representing the changes of plastic contact area…
all macroscopic frictional parameters of the rate and state framework are related to the parameters of the elementary contacts…
We discuss the scaling of the frictional parameters for active faults and landslides."

A micromechanical model of rate and state friction: 1. Static and dynamic sliding, *Perfettini and Molinari*, 2017 (NO pictures!)

theory underlies numerical earthquake cycle & rupture models

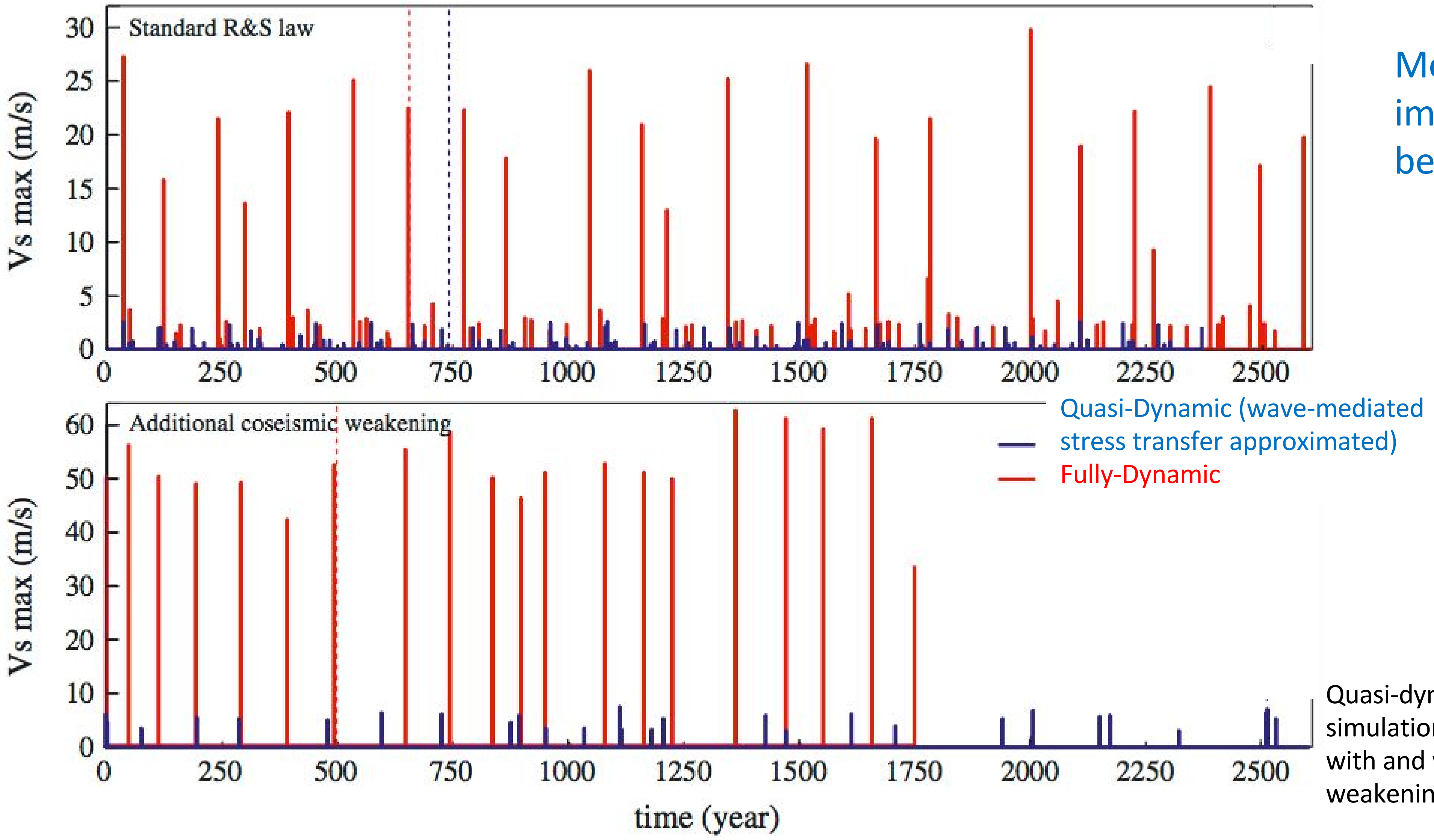

Model assumptions implications need to be understood.

Quasi-dynamic versus fully dynamic simulations of earthquakes and aseismic slip with and without enhanced coseismic weakening, *Thomas, Lapusta et al.*, 2014

numerical models show patch size distribution creates a richness of slip behaviors

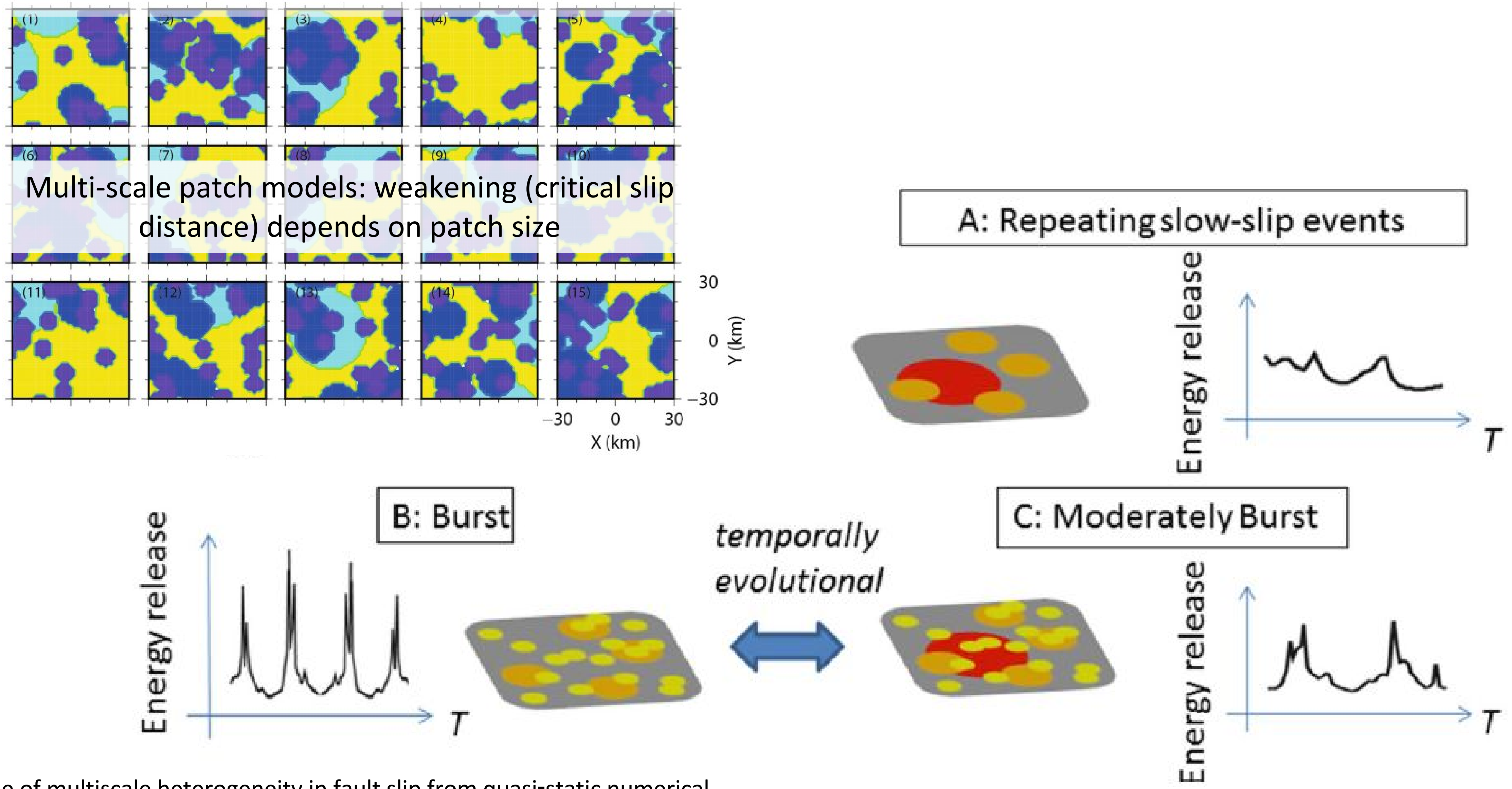

Role of multiscale heterogeneity in fault slip from quasi-static numerical simulations, *Aochi & Ide*, 2017

Forefront science enables safe energy production.

enhanced geothermal energy requires controlled micro-earthquake activity

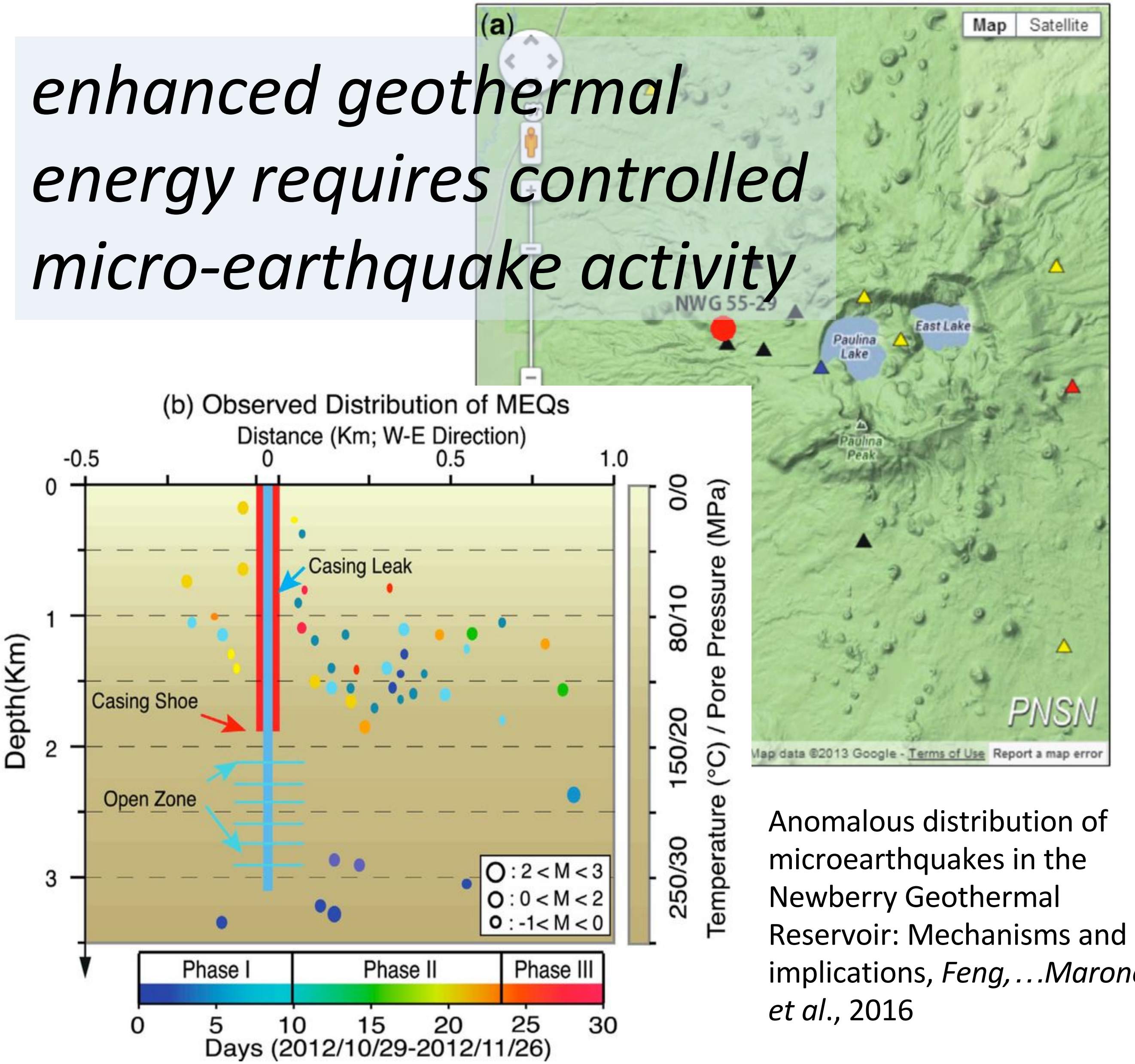

Anomalous distribution of microearthquakes in the Newberry Geothermal Reservoir: Mechanisms and implications, *Feng,…Marone, et al.*, 2016

lab measurements show stability varies with pore pressure changes

enhanced geothermal energy requires controlled micro-earthquake activity

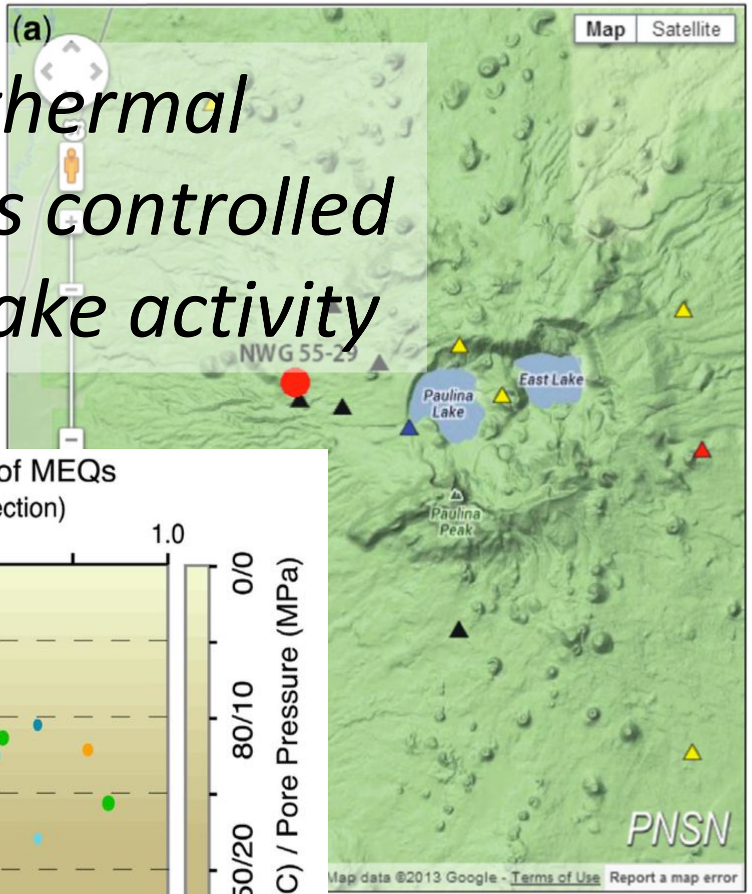

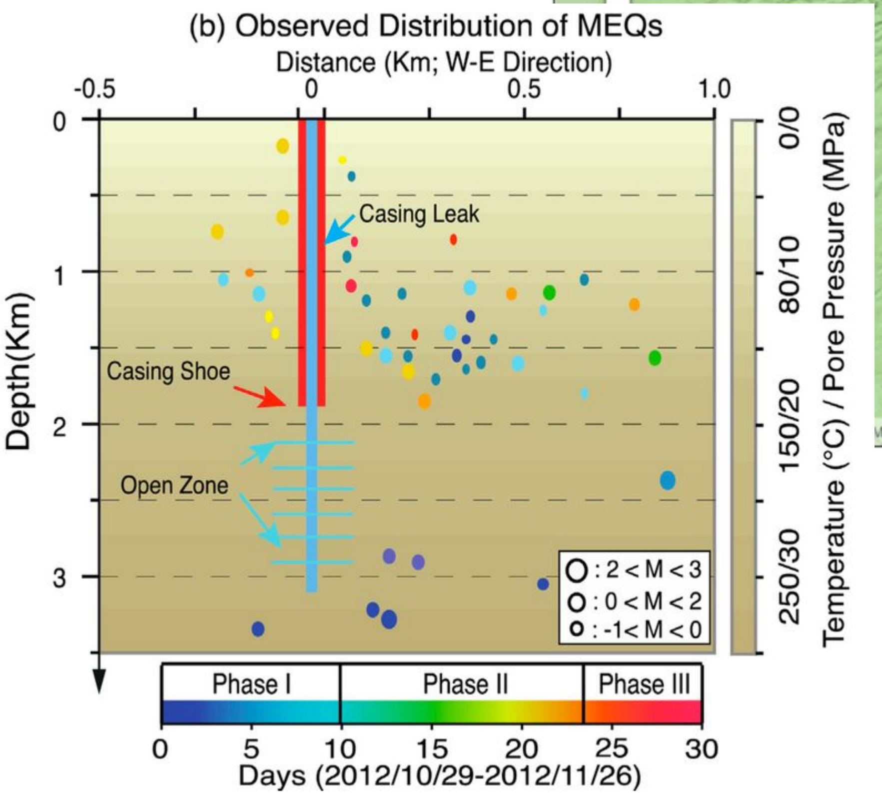

Anomalous distribution of microearthquakes in the Newberry Geothermal Reservoir: Mechanisms and implications, *Feng,…Marone, et al.*, 2016

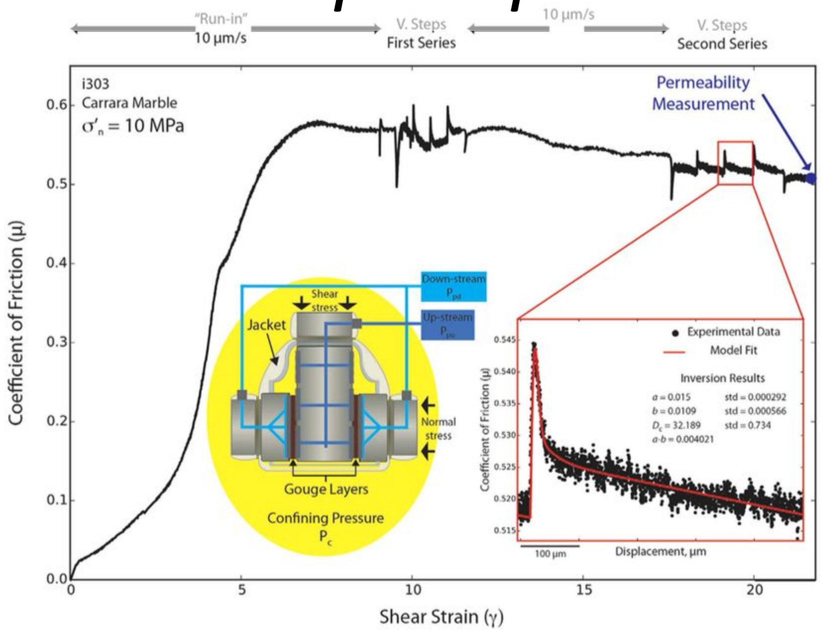

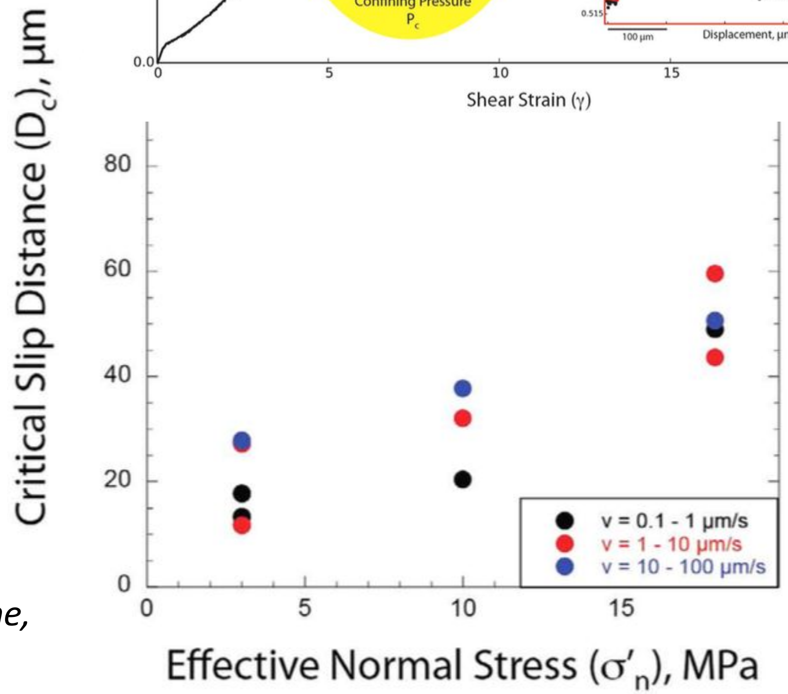

The role of fluid pressure in induced vs. triggered seismicity: insights from rock deformation experiments on carbonates, *Scuderi and Collettini*, 2016

dry lab experiments show creep also contributes to seismicity migration

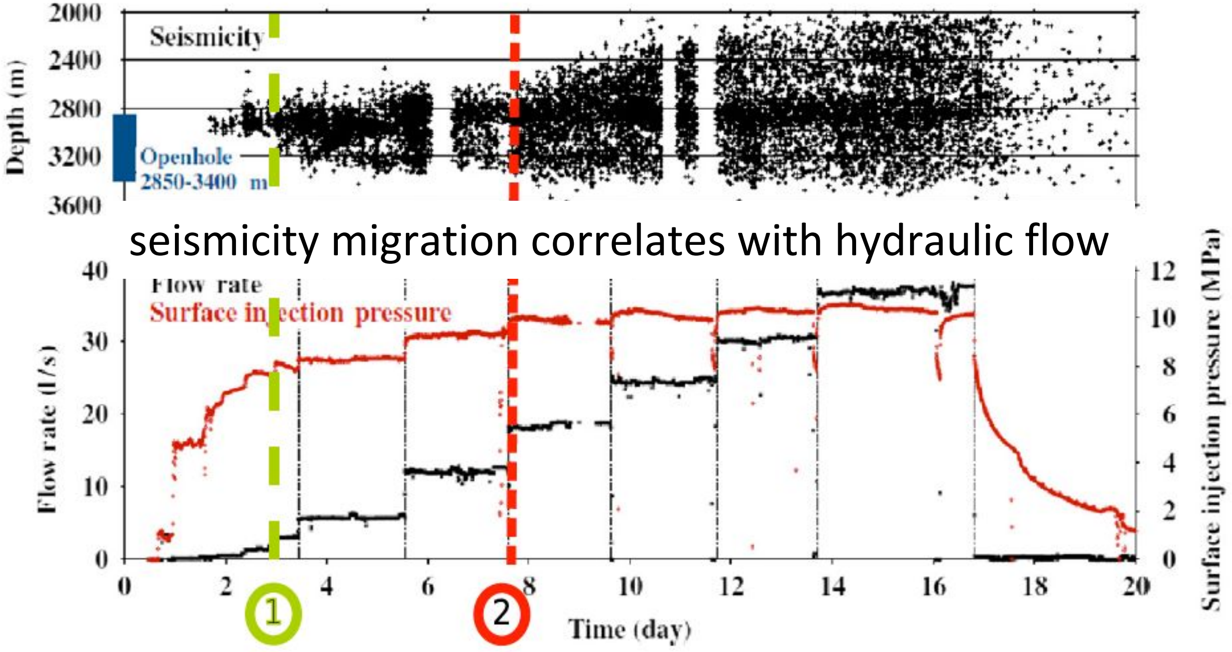

seismicity migration correlates with hydraulic flow

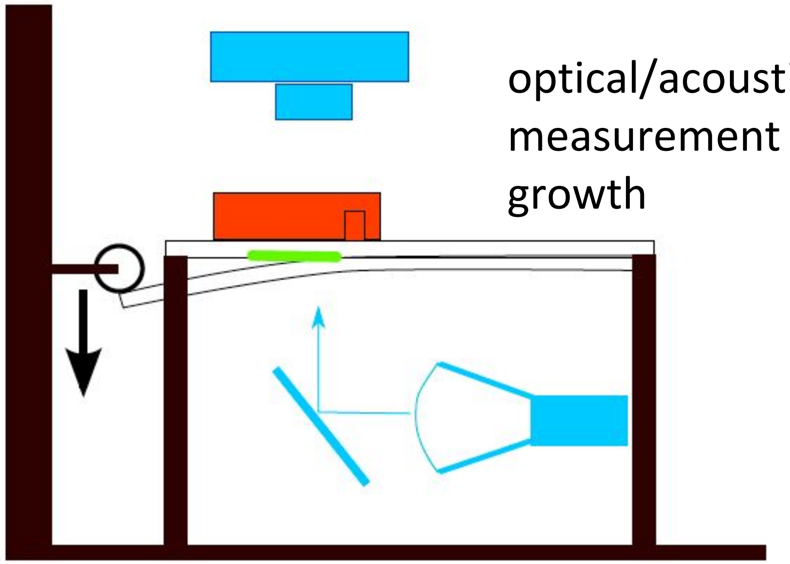

optical/acoustic measurement of dry crack growth

Induced seismicity in EGS reservoir: the creep route, *Schmittbuhl et al.*, 2014

dry lab experiments show creep also contributes to seismicity migration

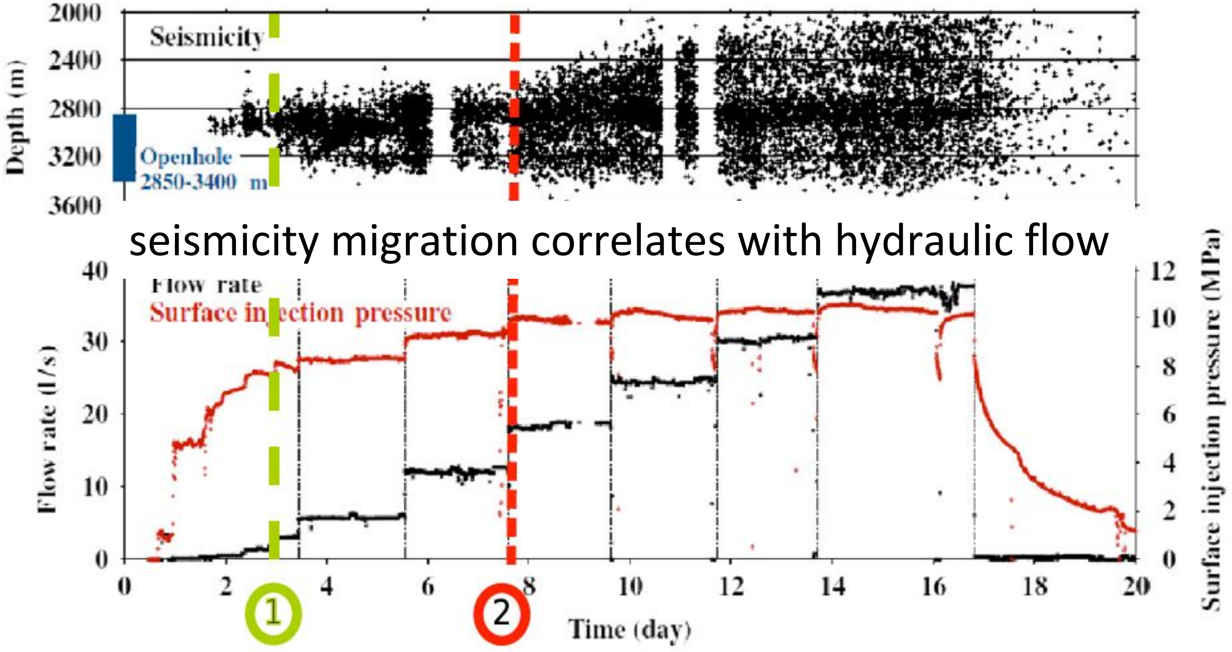

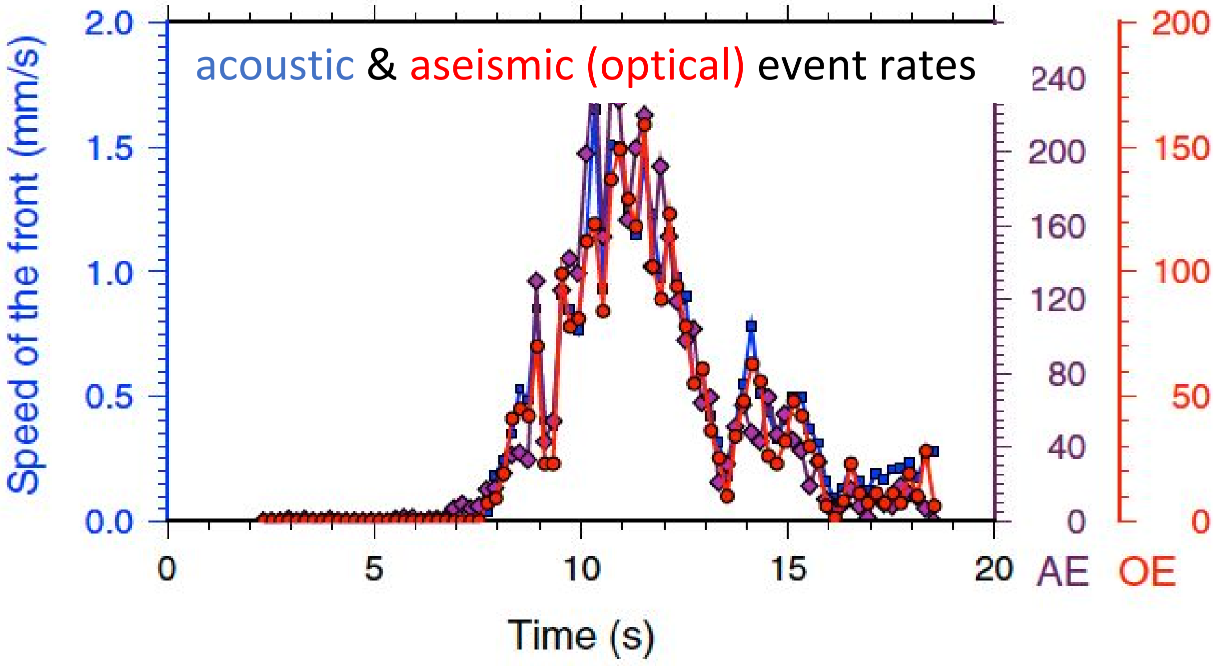

acoustic emission sources ◯ migrate along crack front

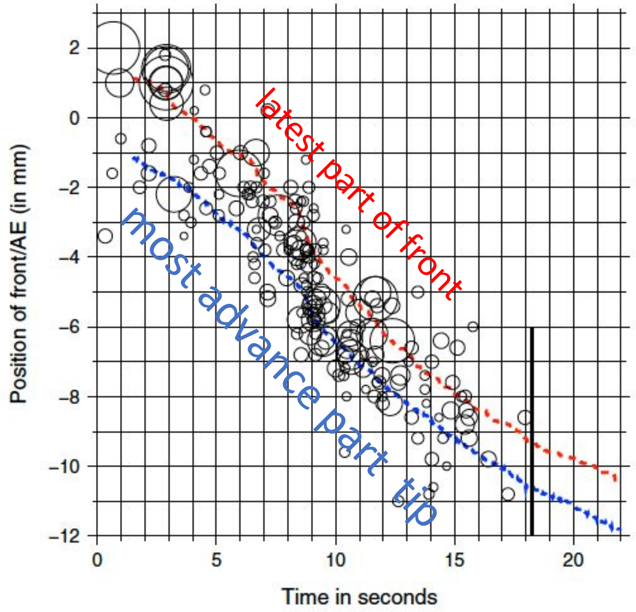

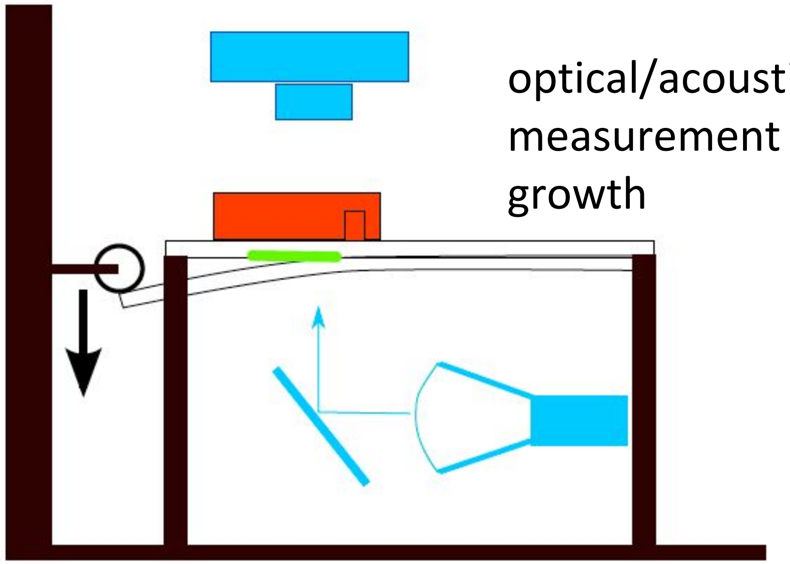

optical/acoustic measurement of dry crack growth

Understood signs of restlessness emerge

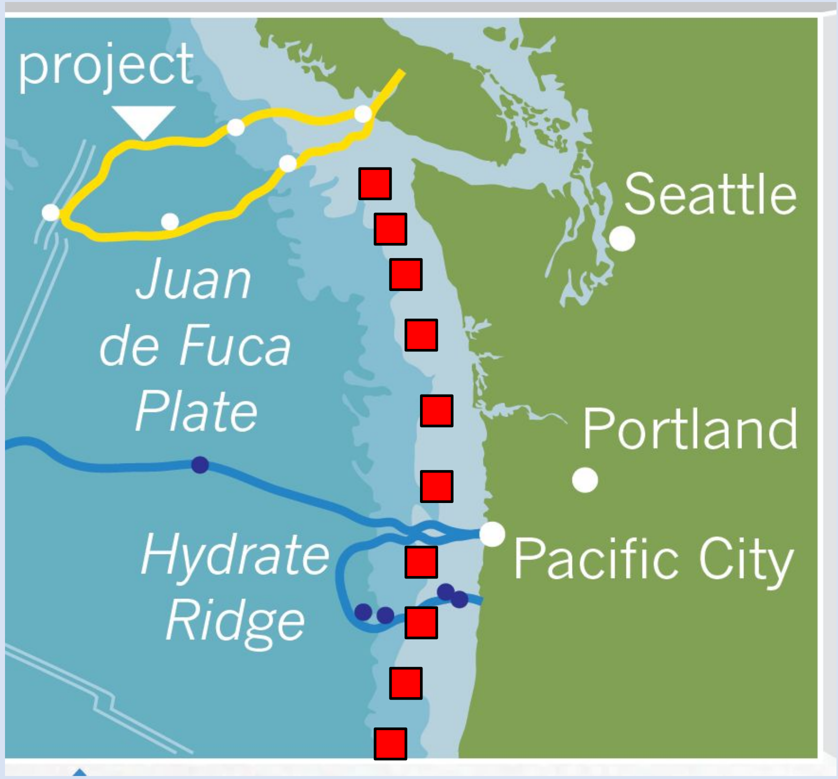

Aware citizens note a cluster of M4-6 earthquakes offshore lasting several weeks. Scientists are confident that the earthquakes are occurring along the plate-interface below where the seafloor is slowly deforming, alerting them to building stresses. Scientists notify emergency managers and public officials, who begin to prepare.

Tantalizing scientific evidence of VERY early warning.

Foreshocks and slow slip commence 50 hours before the 2011 M9 Tohoku earthquake

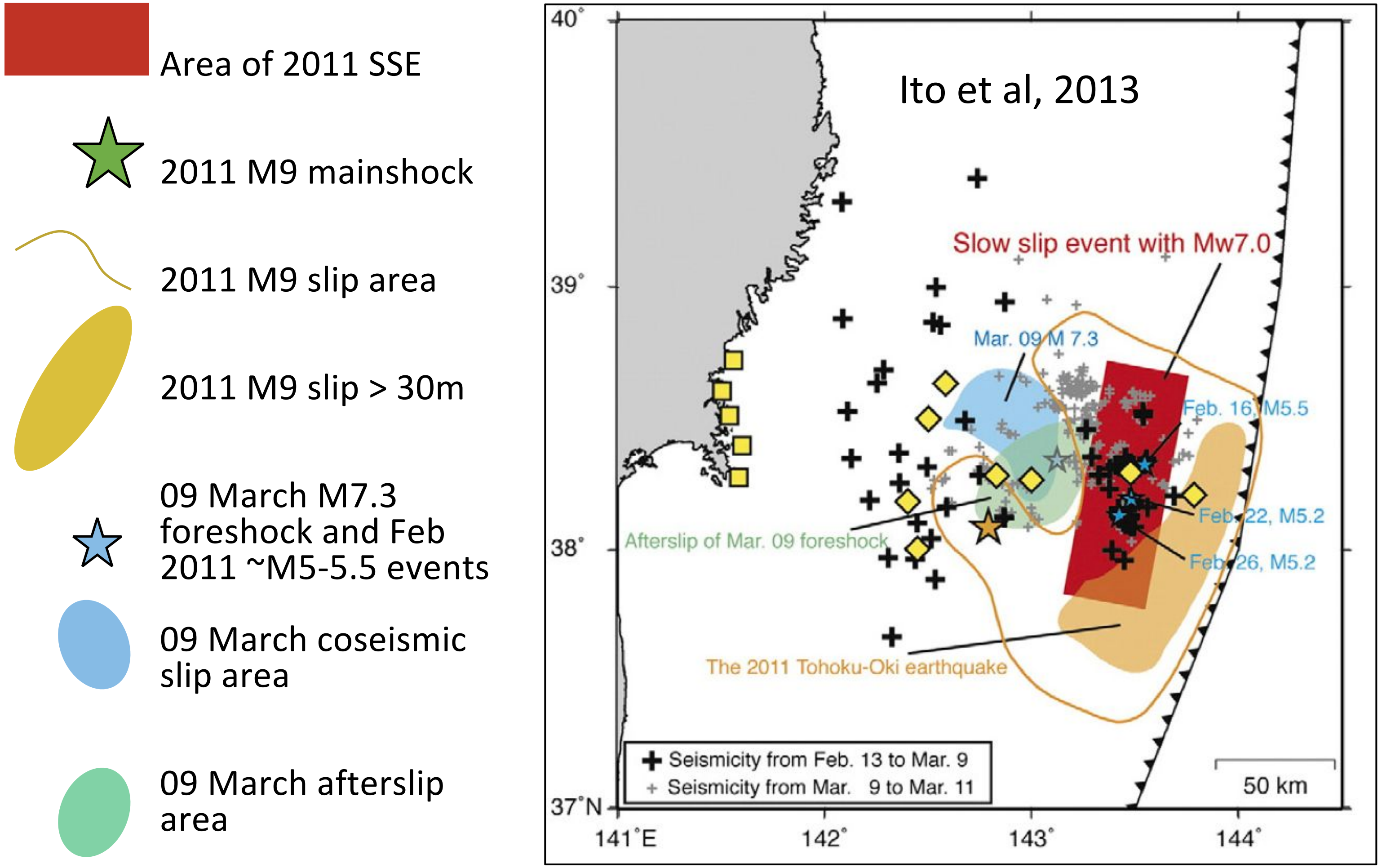

Scientific evidence for VERY early warning.

M6.2 foreshock coseismic and afterslip trigger M7.0 Kumamoto earthquake, revealed in foreshock migration patterns.

Foreshock migration preceding the 2016 Mw 7.0 Kumamoto earthquake, Japan, *Kato et al.*, 2016

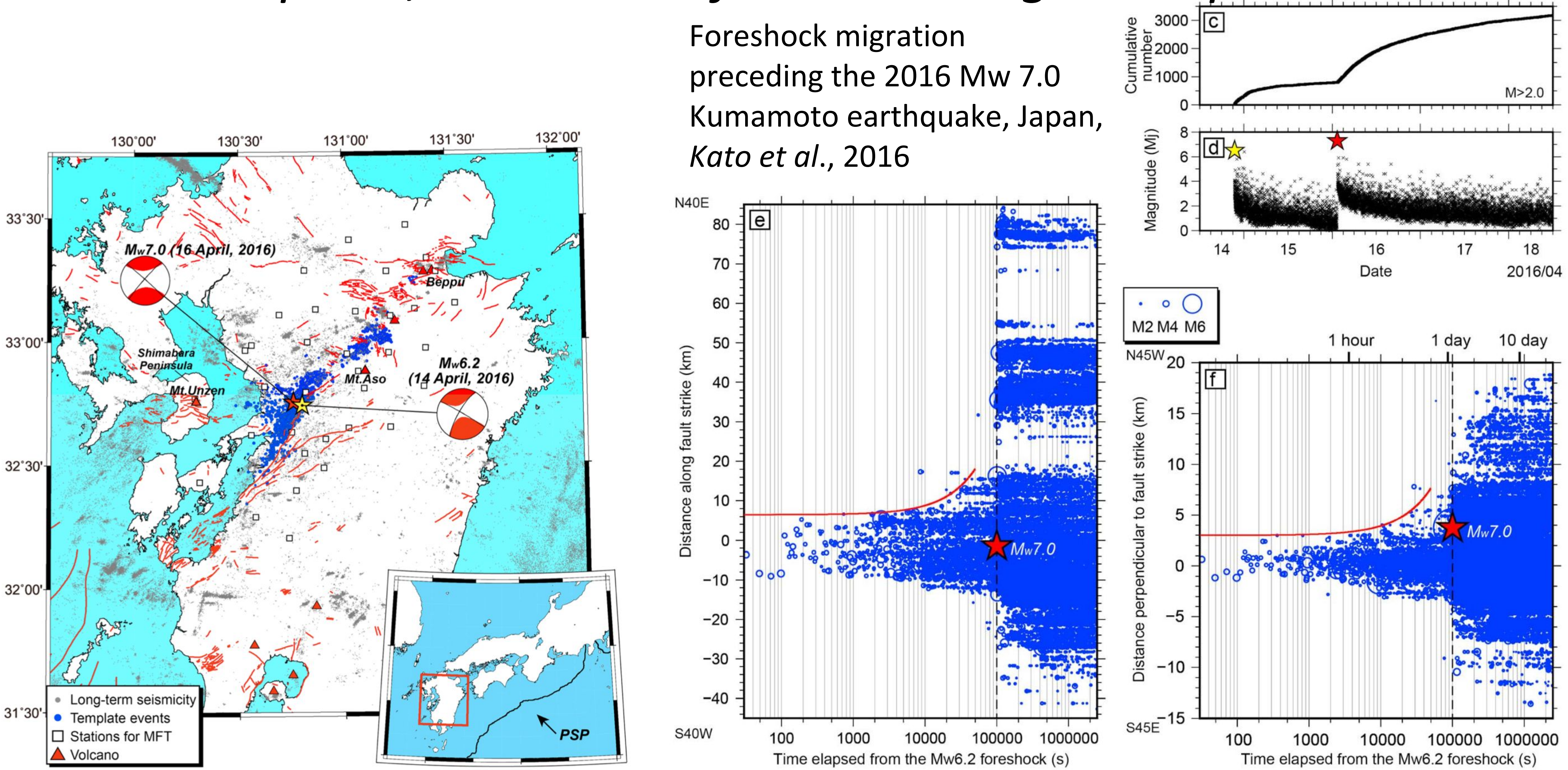

precursory intraplate earthquake rate increases synchronize with interplate foreshocks

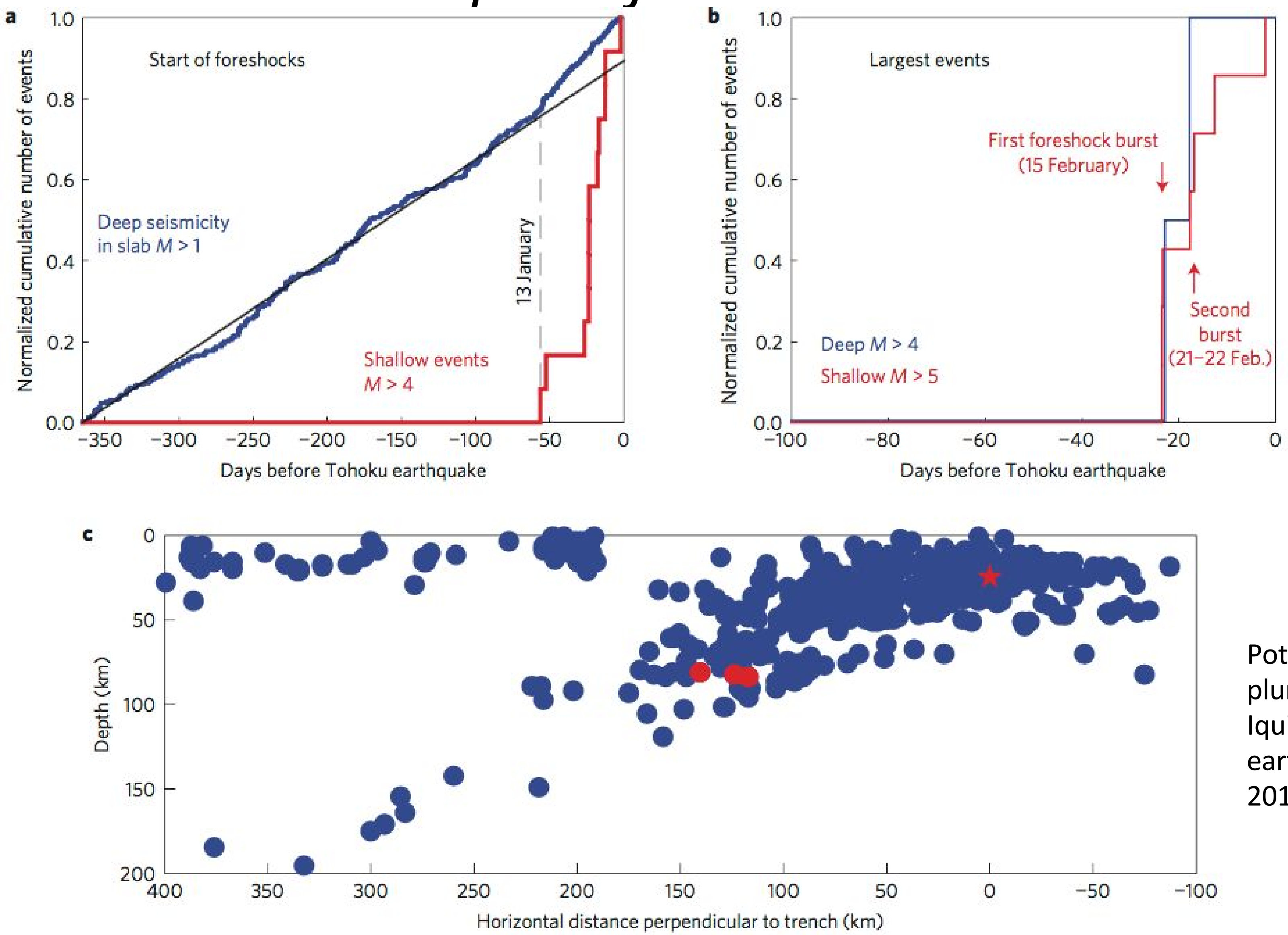

Potential slab deformation and plunge prior to the Tohoku, Iquique and Maule earthquakes, *Bouchon et al.*, 2016

The public is informed as a great earthquake unfolds.

Several days later, nearly two minutes of violent ground shaking awakens the entire region, as the Earth unleashes a M9.1 earthquake. The offshore-onshore earthquake early warning system accurately estimates the intensity of coming strong shaking, giving citizens time to take cover and businesses and infrastructure operators time to shut down operations safely.

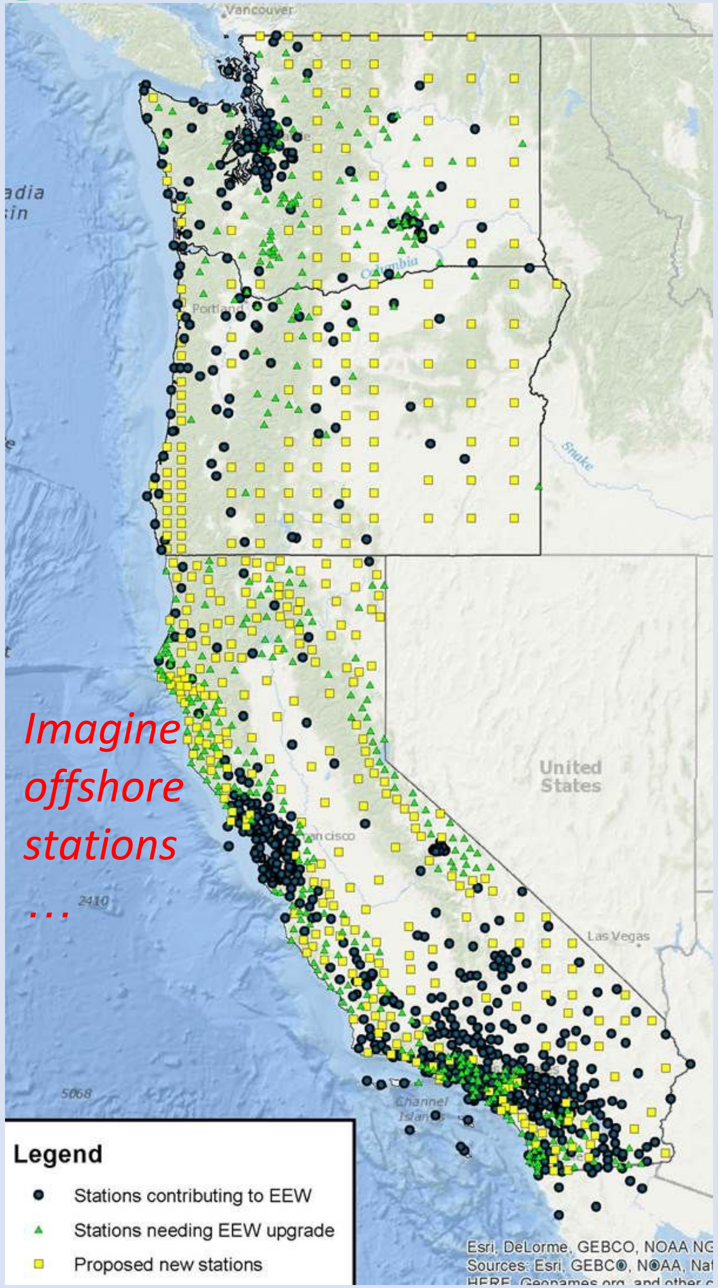

Science interfaces with real-world affairs.

telecommunications, politics, public accountability

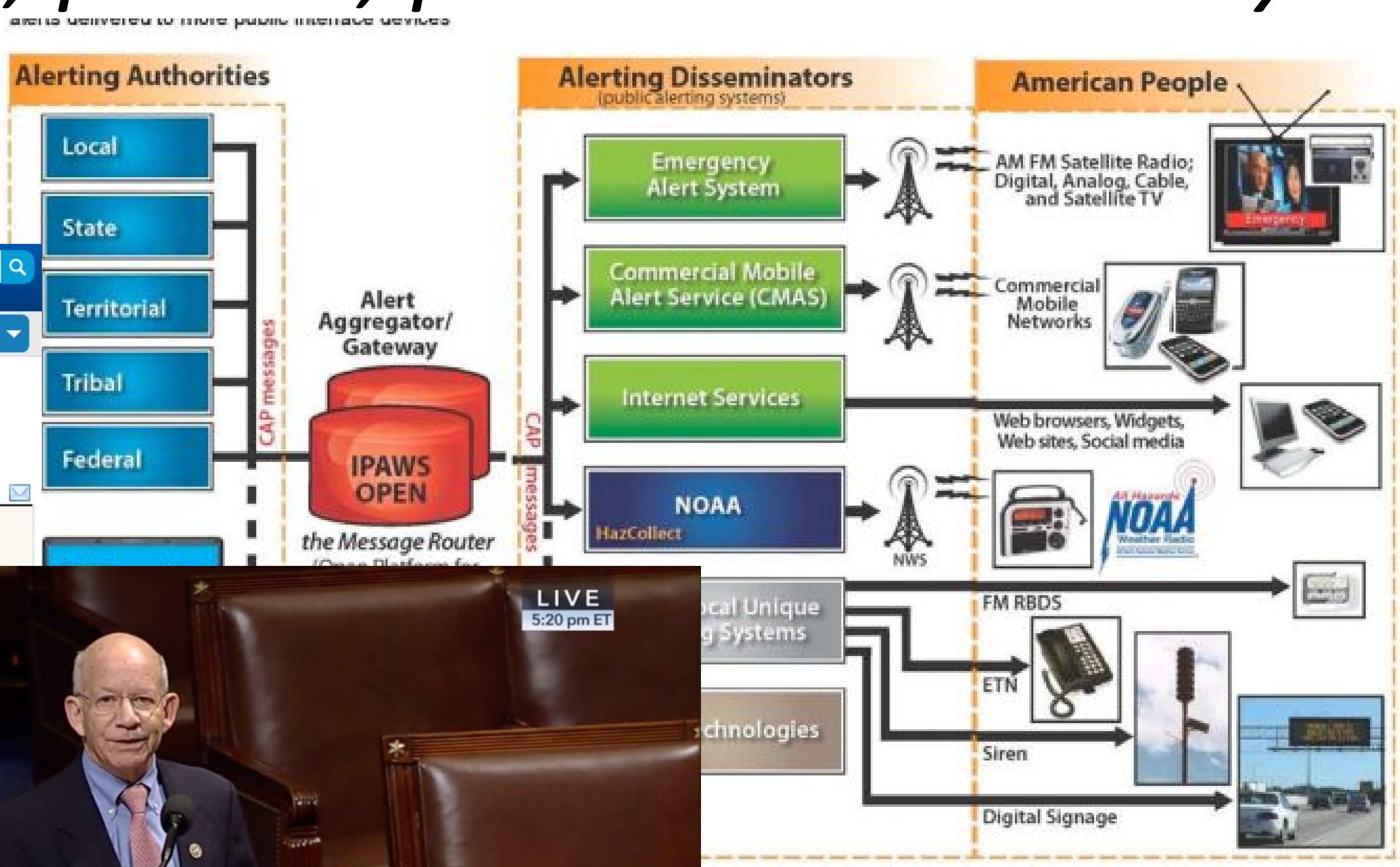

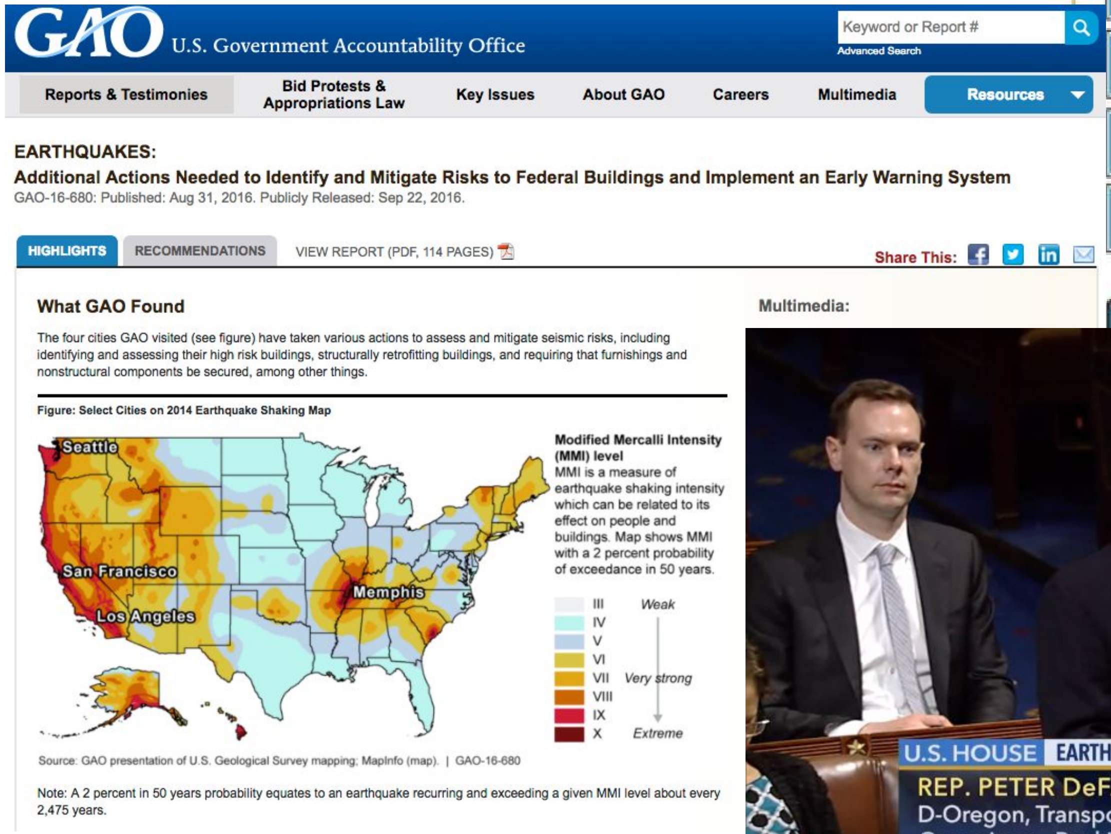

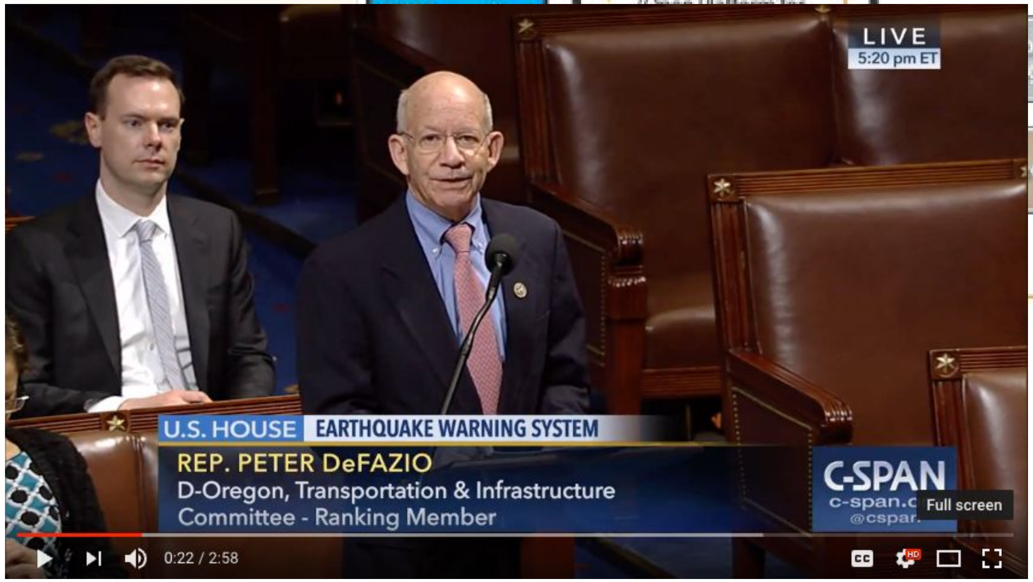

& new technologies that open scientific frontiers

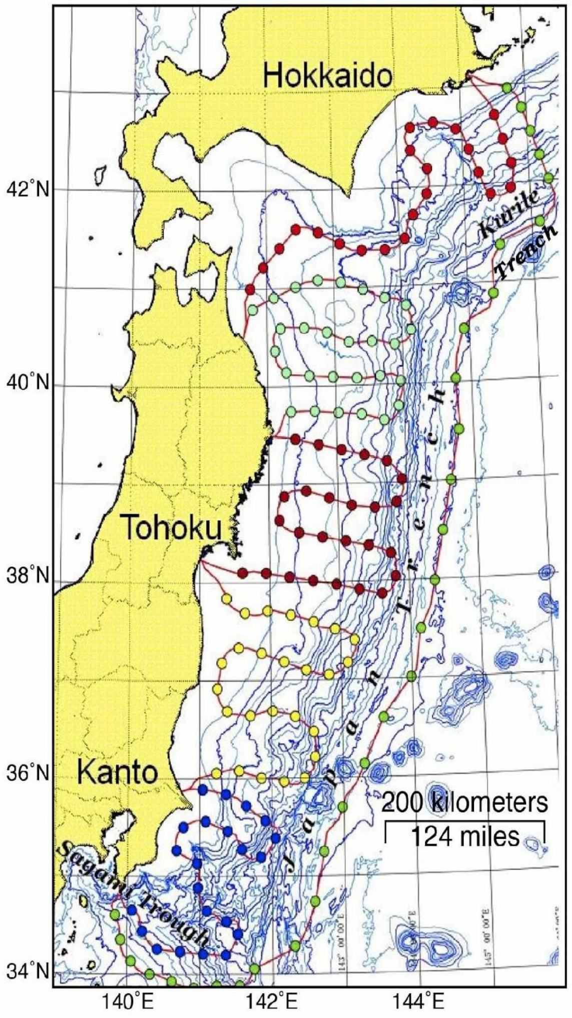

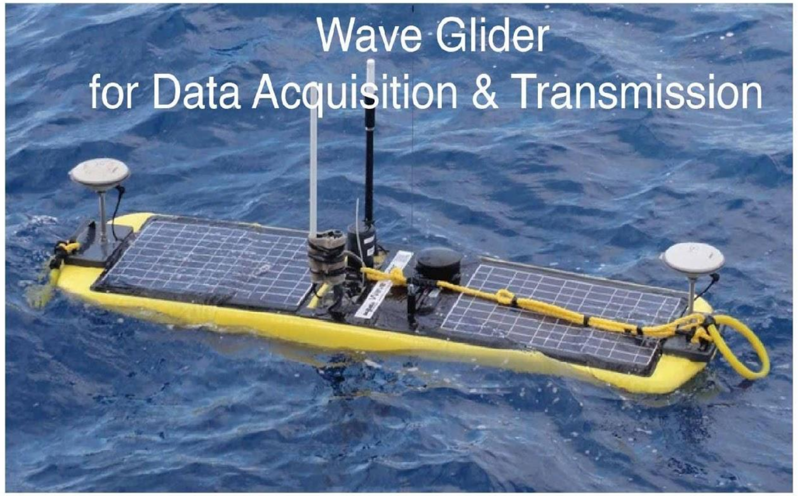

Data Transmission Modems

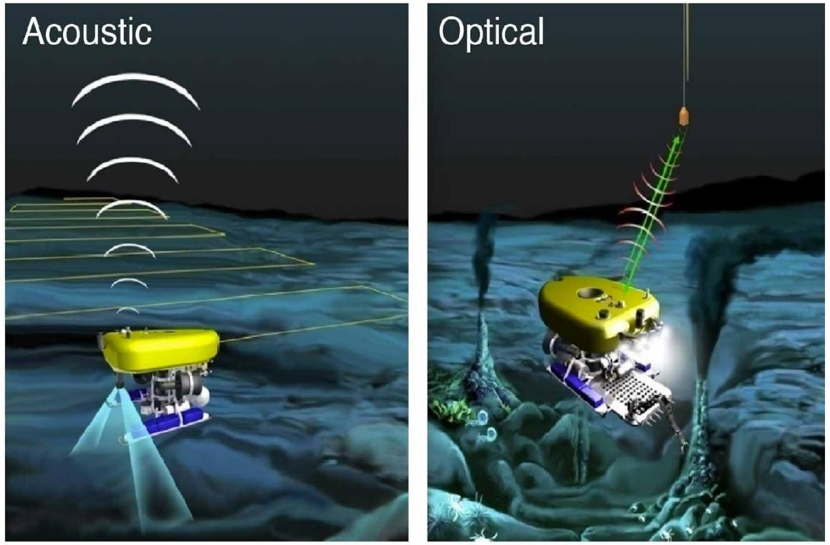

Shaking depends on source scaling.

evolving radiated energies reveals stress drop variability

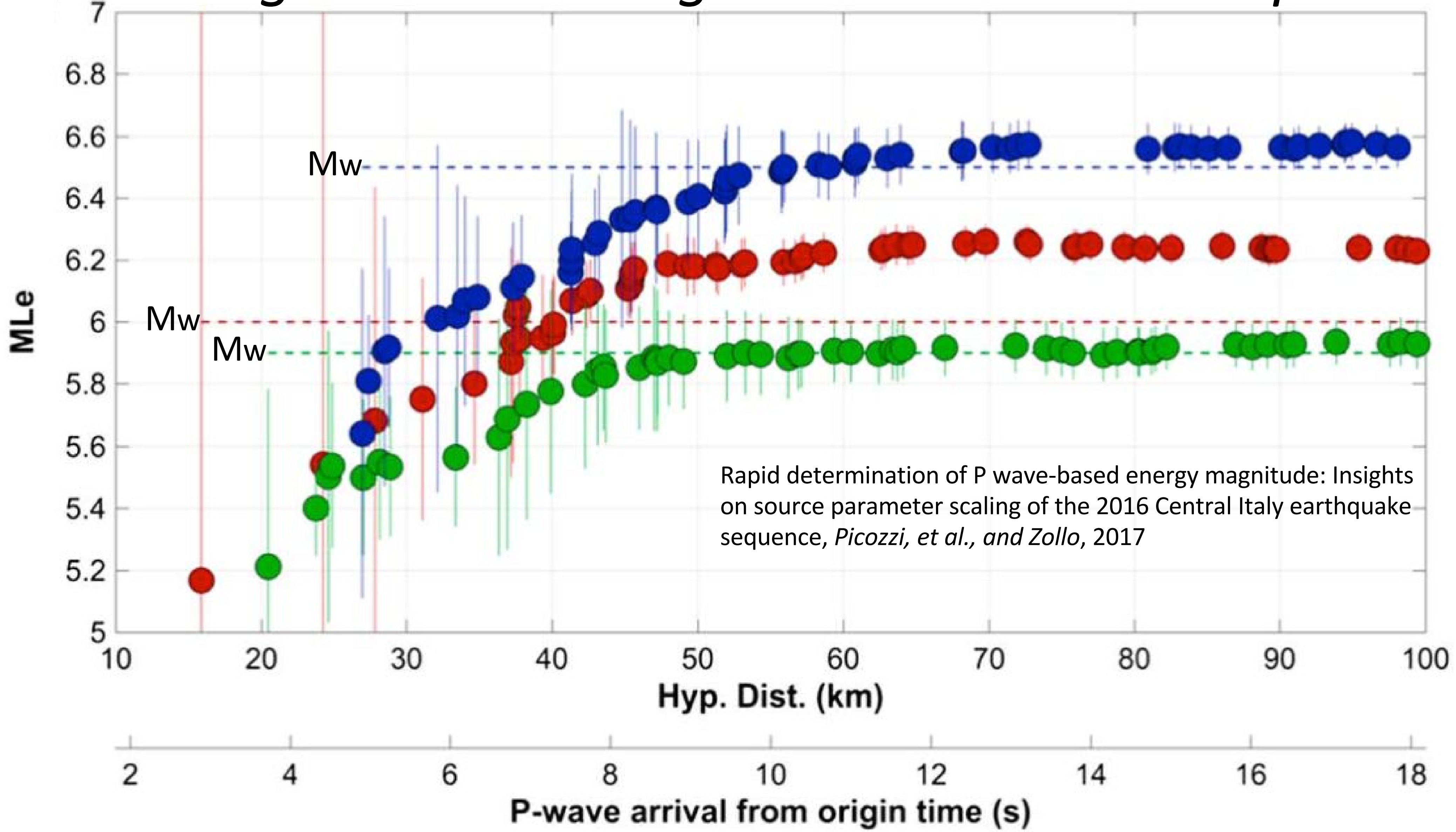

'departure time' vs magnitude scaling implies ruptures aren't initially deterministic, but size soon becomes predictable

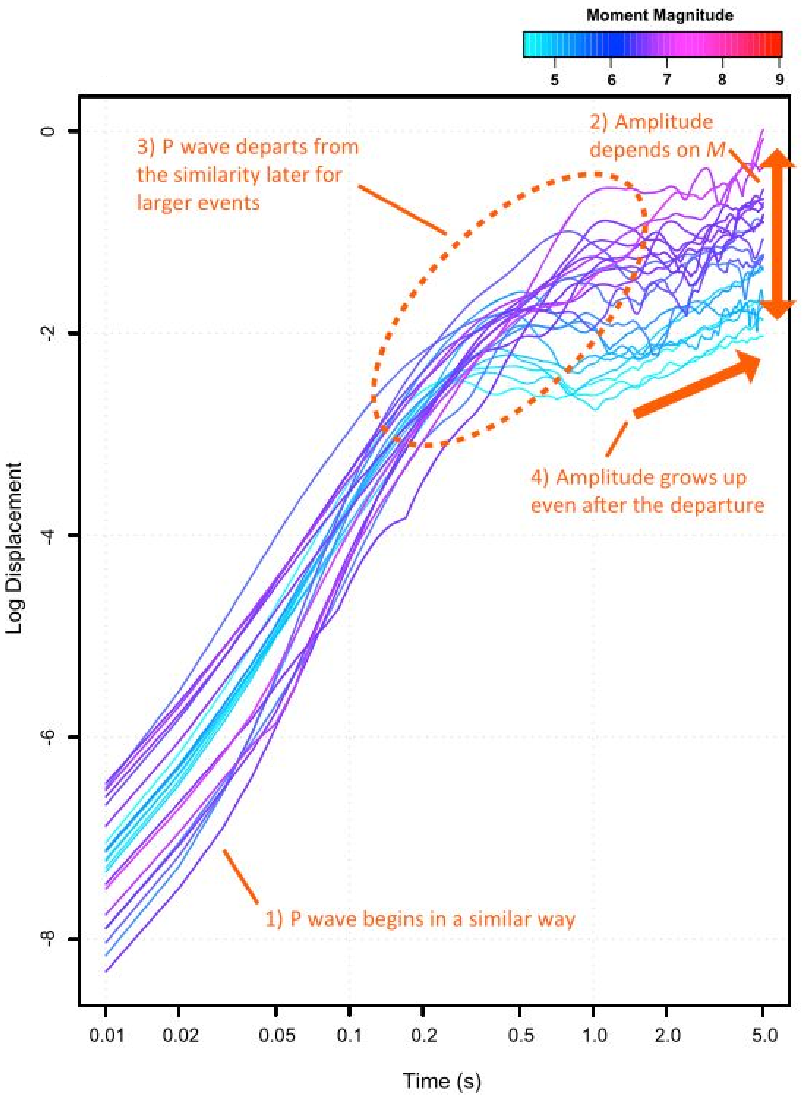

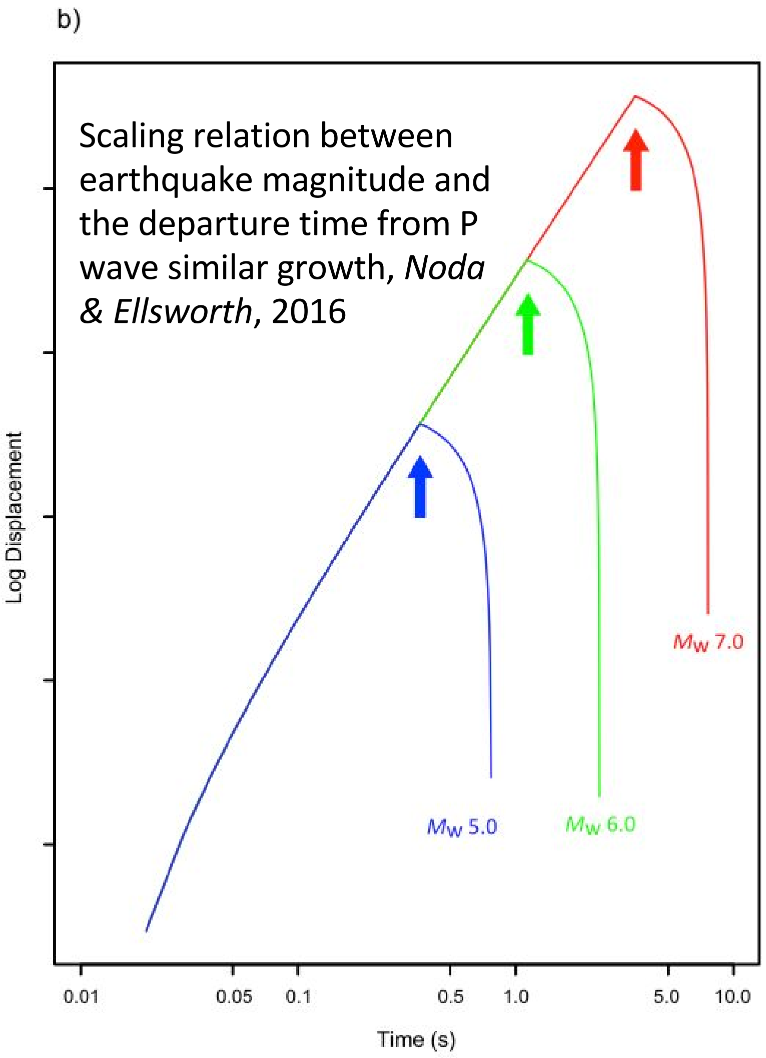

‘departure time’ vs magnitude scaling implies ruptures aren’t initially deterministic, but size soon becomes predictable

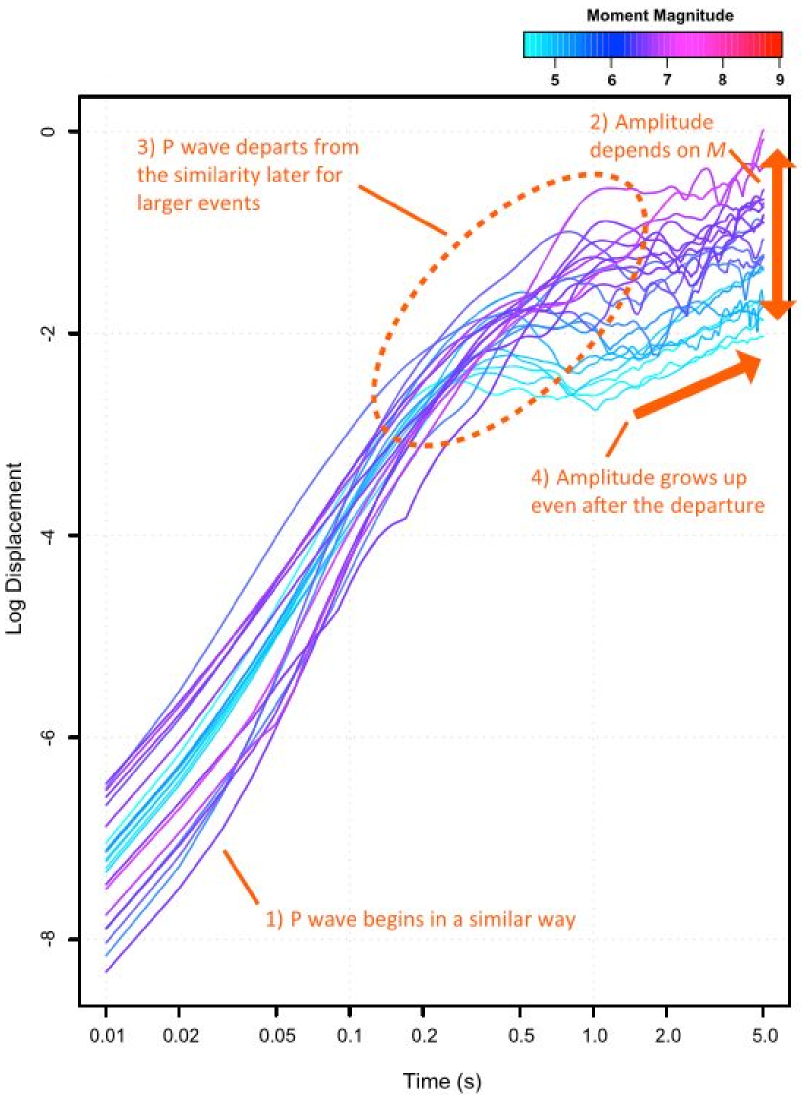

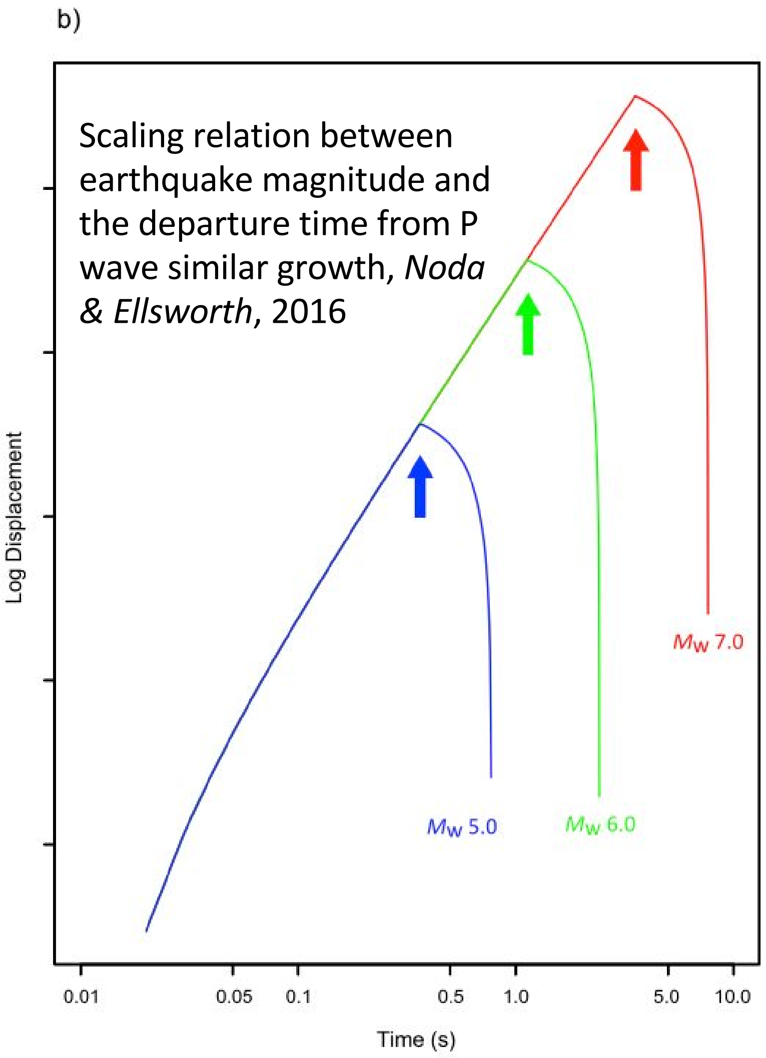

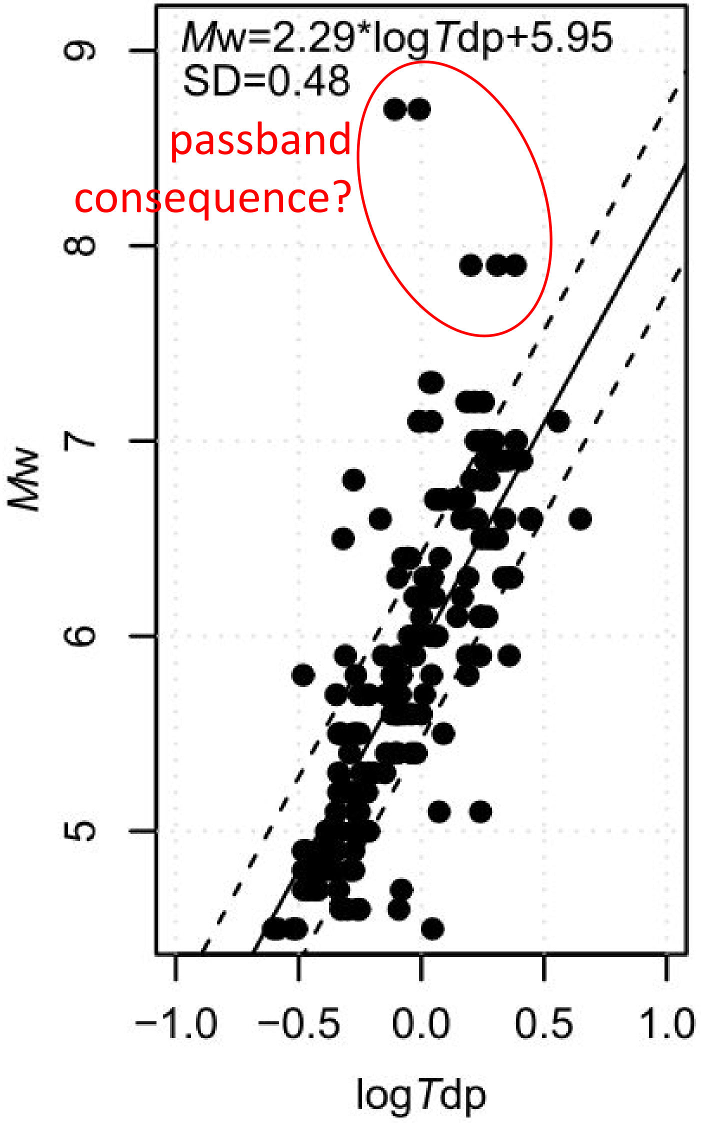

uncertainties & trade-offs often map into over-estimated hazard

M6.0 Parkfield Earthquake – 13 Slip Models

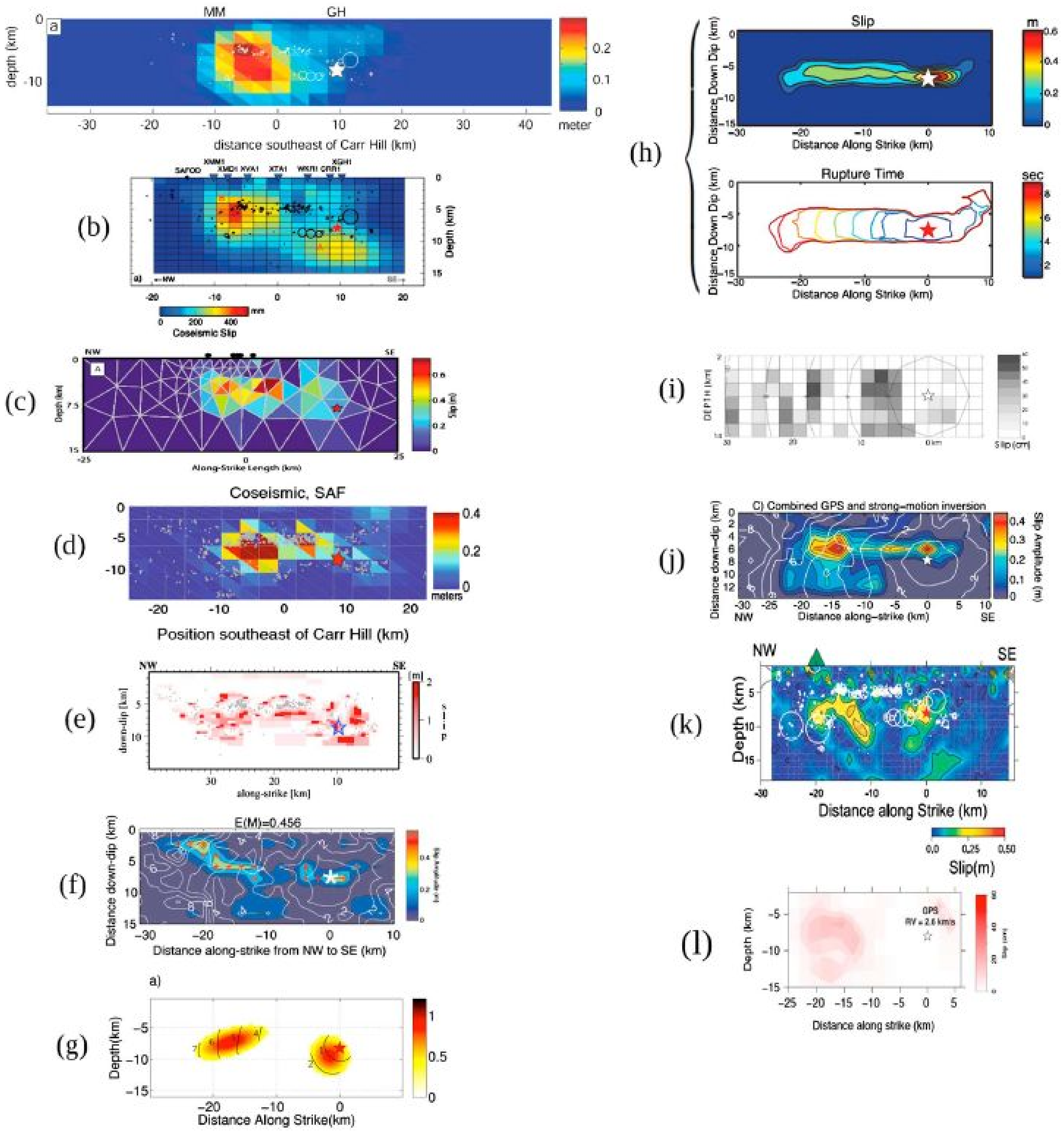

Resolution/Trade-offs of Dynamic Rupture Properties

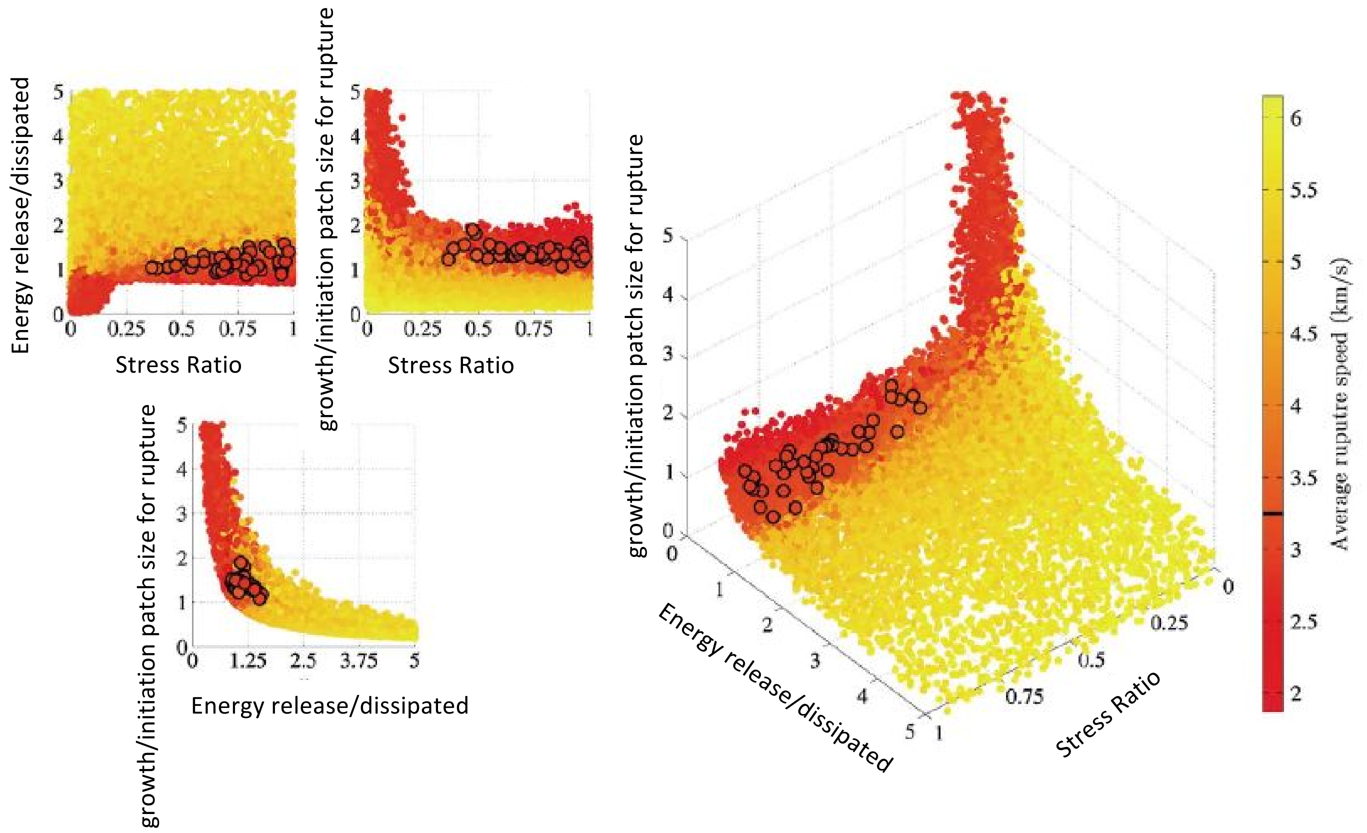

Inversion for the physical parameters that control the source dynamics of the 2004 Parkfield earthquake, *Twardzik, Das & Madariaga*, 2014

Coastal lands are reshaped and flooded, but recovery is effective and efficient.

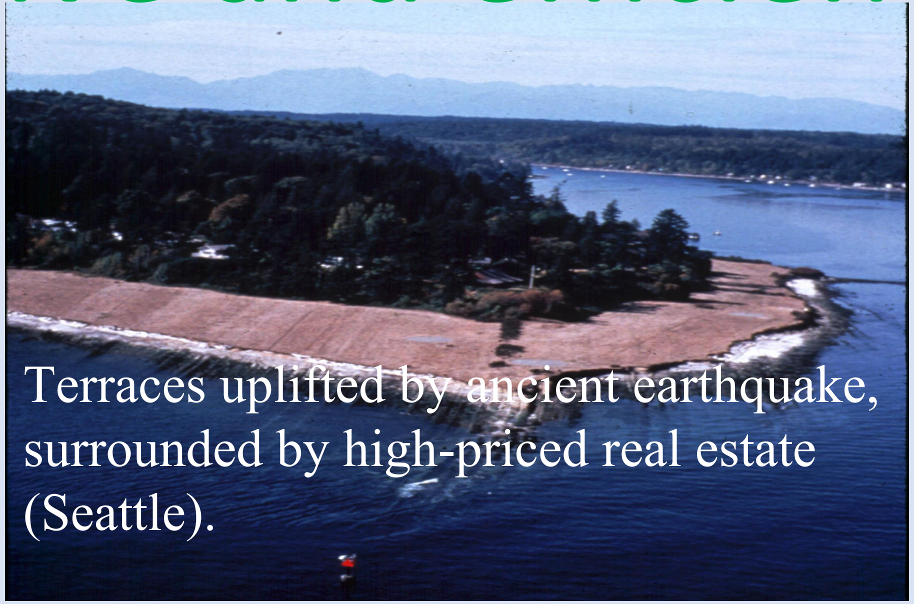

Within minutes, huge tracks of coastal land drop, rivers change course, seawater floods low-lying areas, and coastal wildlife habitats disappear. Tsunami waves carry walls of water stories tall across coastlines. Citizens evacuate to safety. Initial land-level change and tsunami forecasts are updated, feeding into evolving impact assessments and situational awareness. Transportation is rerouted to avoid submerged roads and rails, enabling rapid delivery of relief.

Resilience-building products, underlain by science.

horizontal & vertical tsunami evacuation preparations

scenario inundation maps

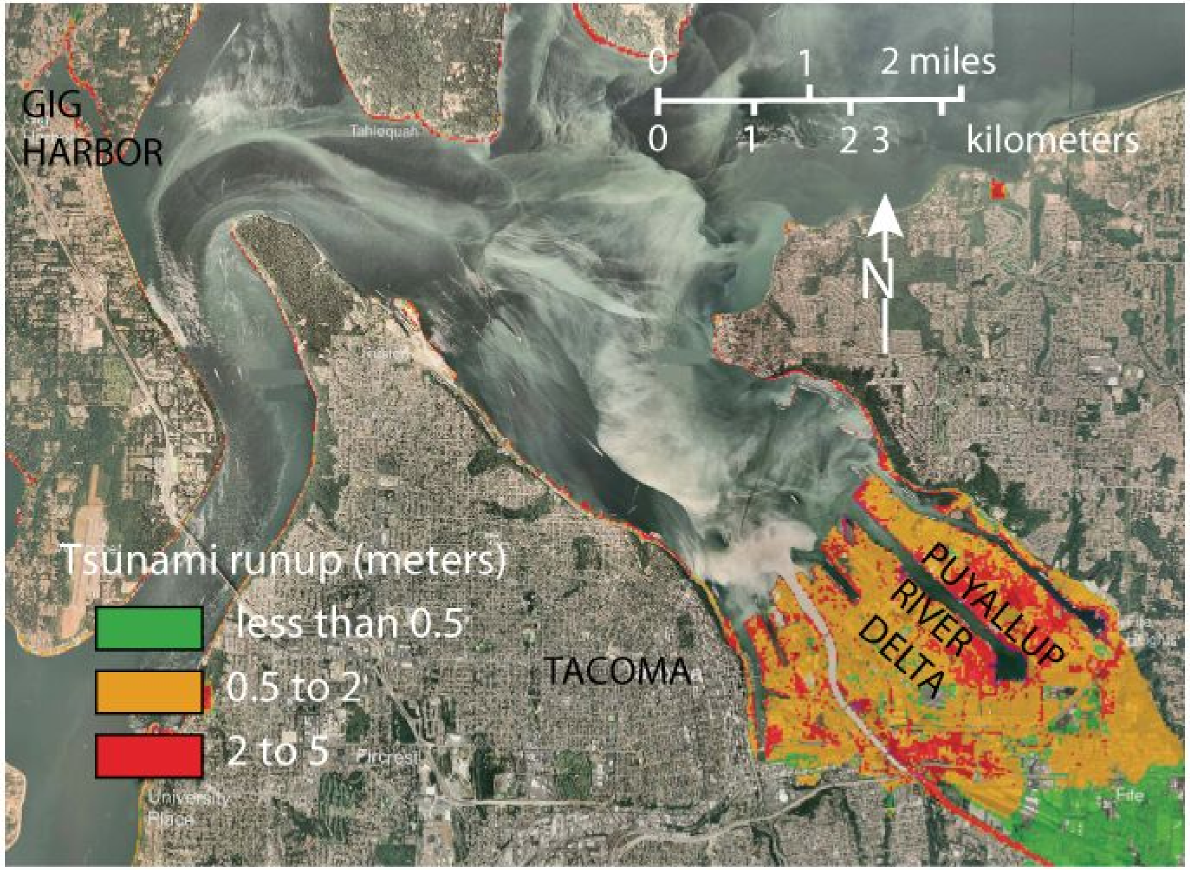

Crustal Tacoma fault earthquake-triggered tsunami maximum inundation reaches ~12 feet, flooding begins in Tacoma area within ~5 min (from WA Dept. of Natural Resources).

probabilistic tsunami wave height assessments

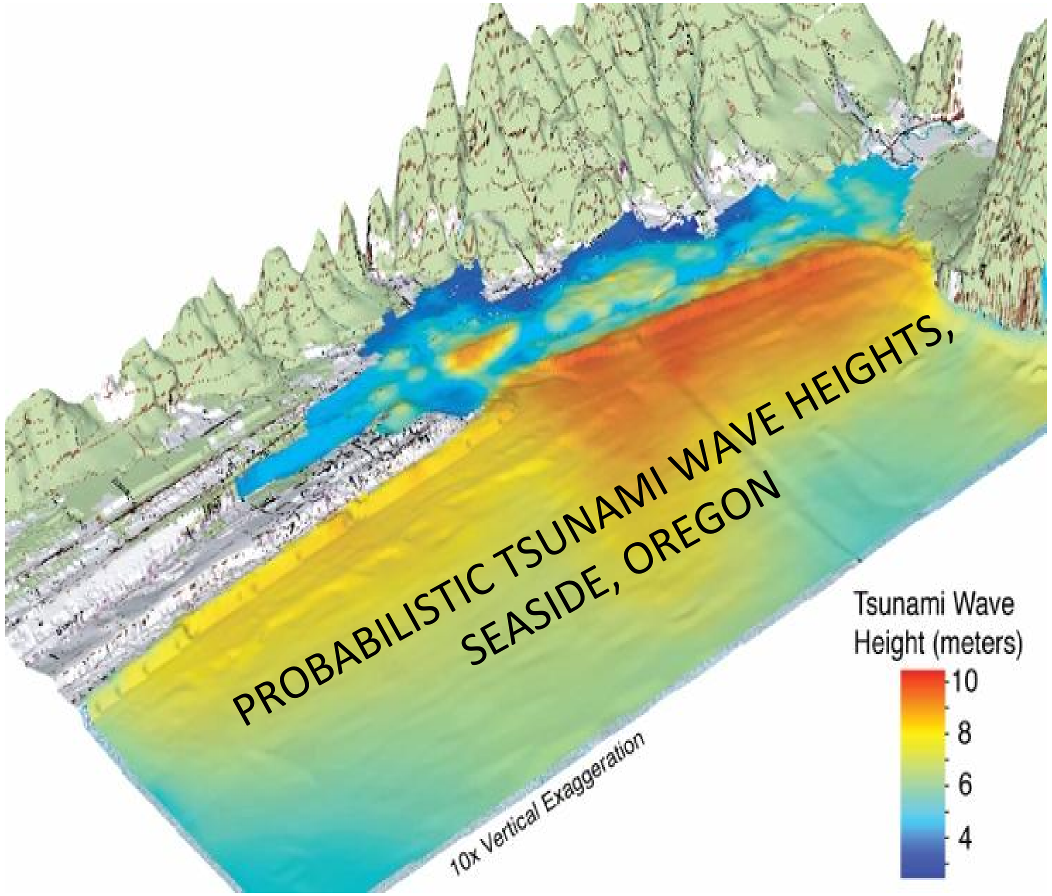

USGS pilot project; lacks splay fault and shaking-triggered landslide sources.

Forefront science & technology will provide initial and updated land-level forecasts.

satellite imagery, data at scales and places not otherwise reachable

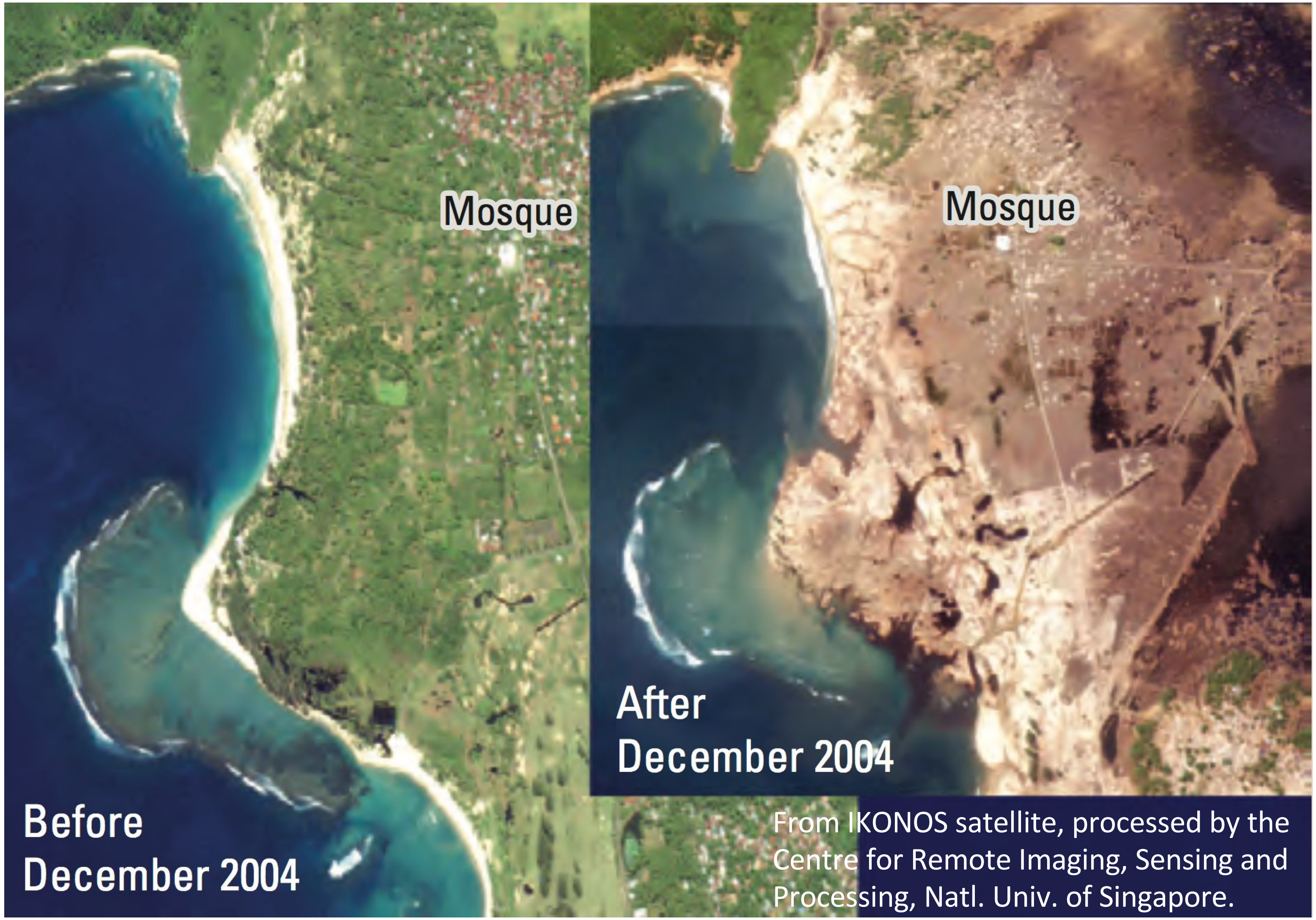

From IKONOS satellite, processed by the Centre for Remote Imaging, Sensing and Processing, Natl. Univ. of Singapore.

new & varied seafloor observations advance tsunami generation understanding

Tohoku shallow slip triggers outer-rise normal aftershocks

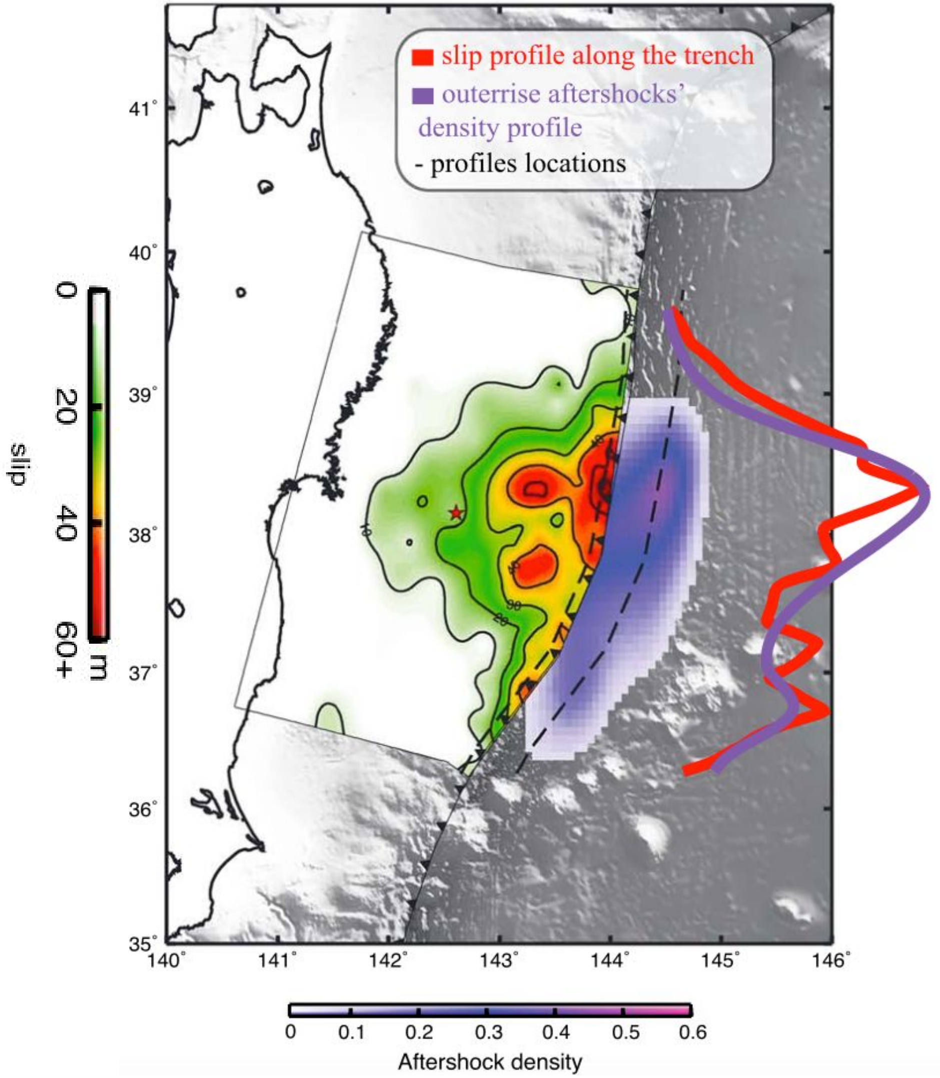

A detailed source model for the *Mw*9.0 Tohoku-Oki earthquake reconciling geodesy, seismology, and tsunami records, Bletery, Sladen et al., 2014

new & varied seafloor observations advance tsunami generation understanding

Tohoku prism normal faulting implies very low dynamic friction (explains large megathrust slip?)

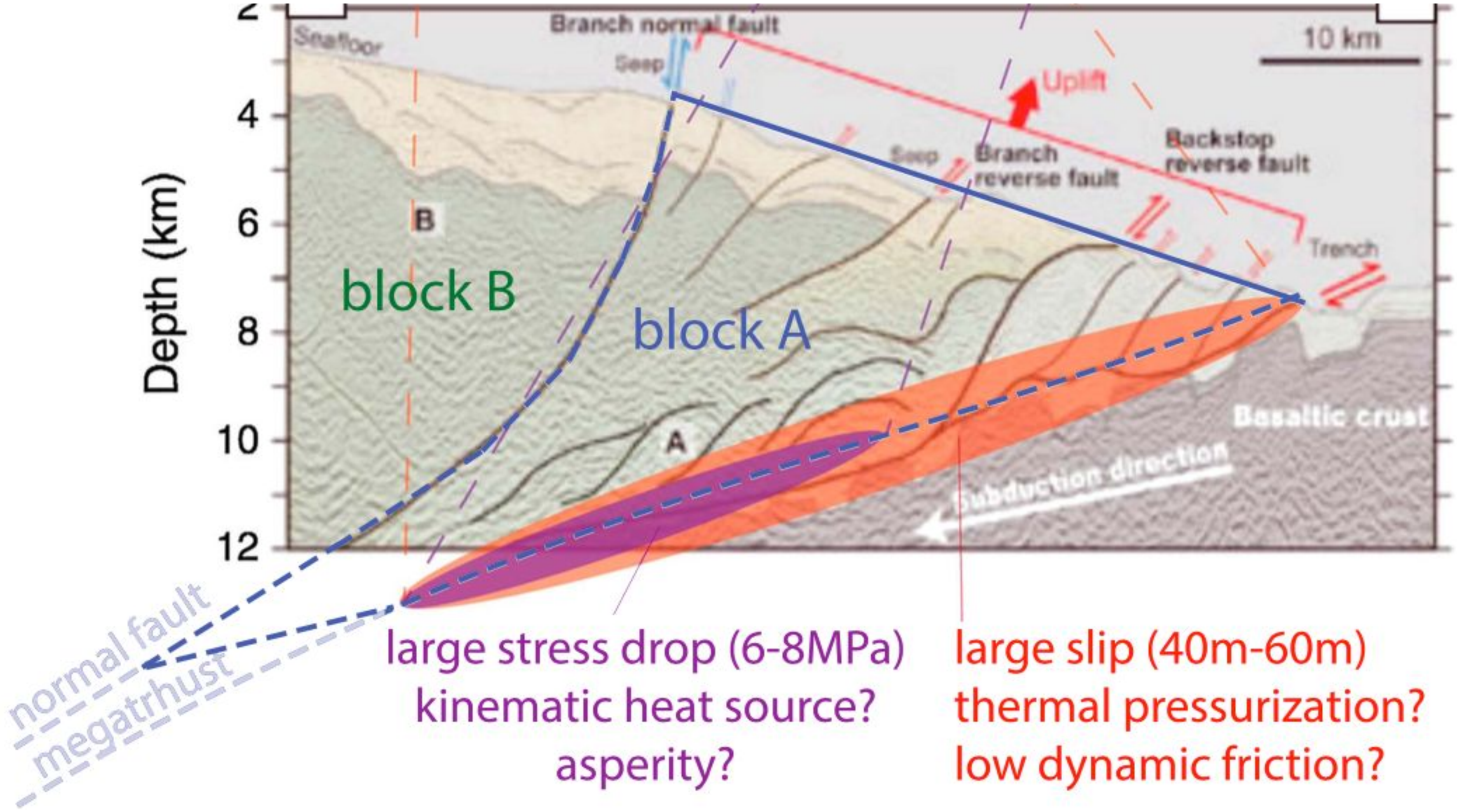

A detailed source model for the *Mw*9.0 Tohoku-Oki earthquake reconciling geodesy, seismology, and tsunami records, Bletery, Sladen et al., 2014

Tohoku shallow slip triggers outer-rise normal aftershocks

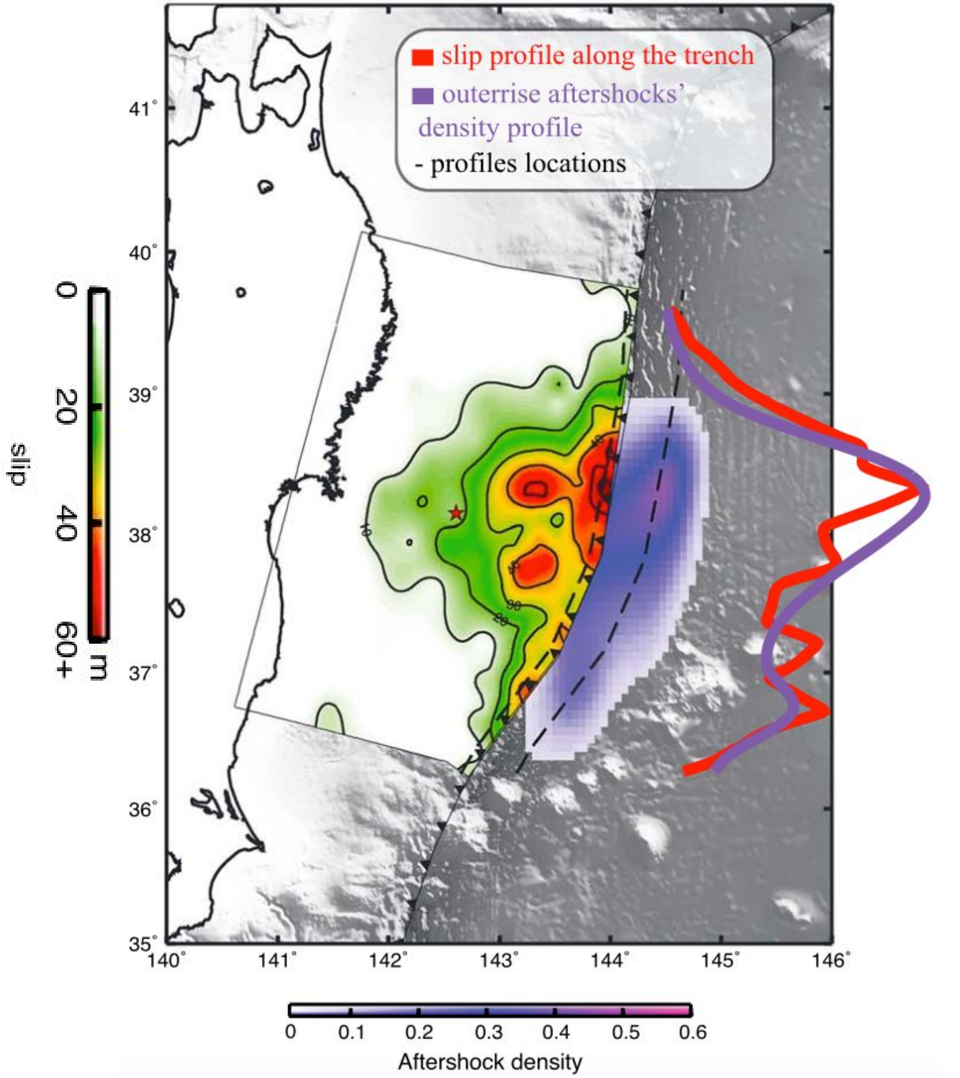

laboratory experiments reveal new rupture processes

Photoelastic Image of Laboratory Slip Event

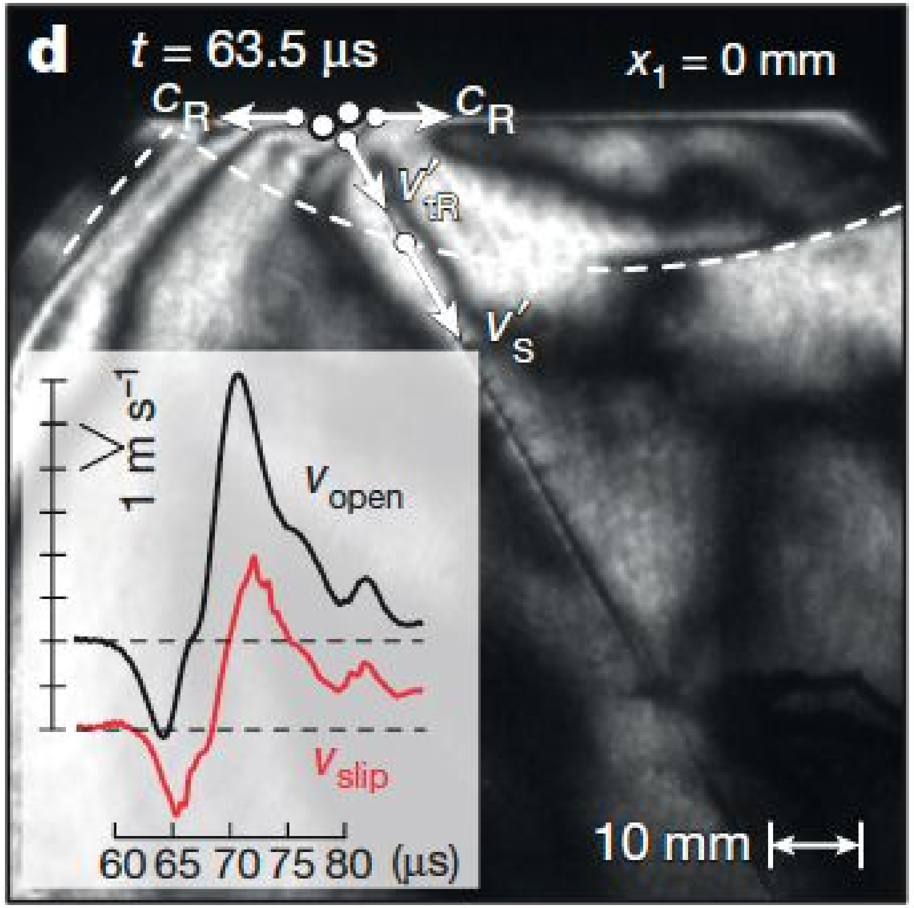

Numerical Model of Laboratory Slip Event

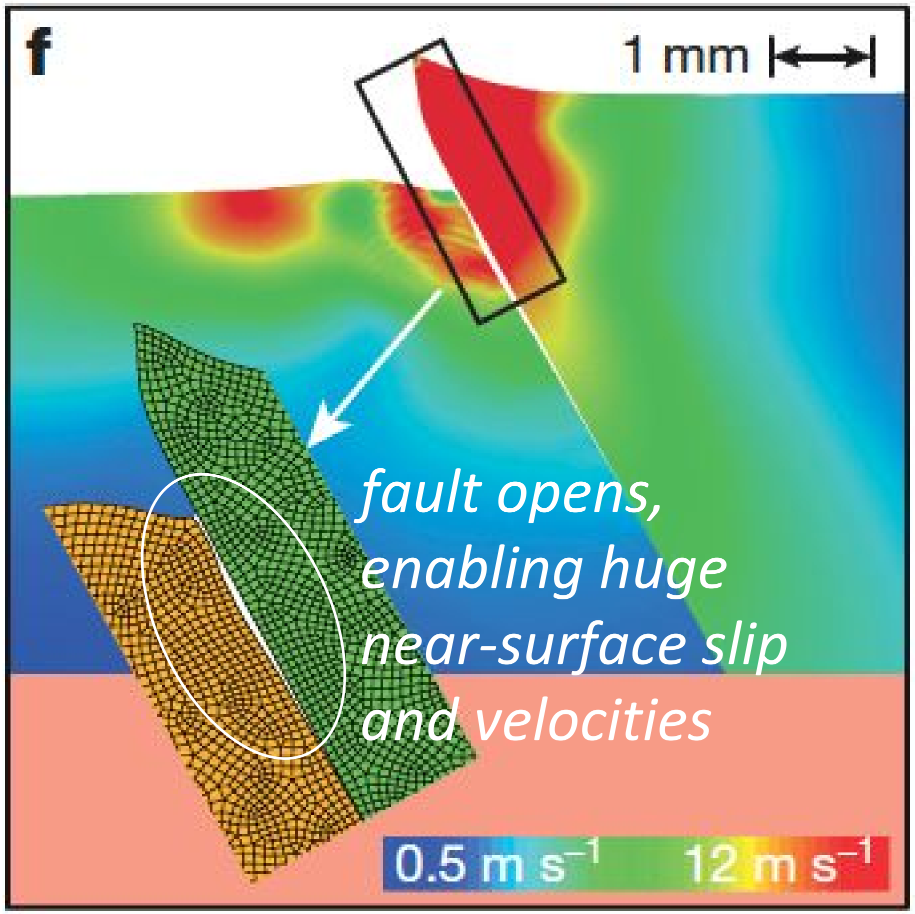

Experimental evidence that thrust earthquake ruptures might open faults, *Gabuchian…Madariaga et al.*, 2017

Success of informed designs/policies is proven.

Neighborhood-scale Probabilistic Shaking

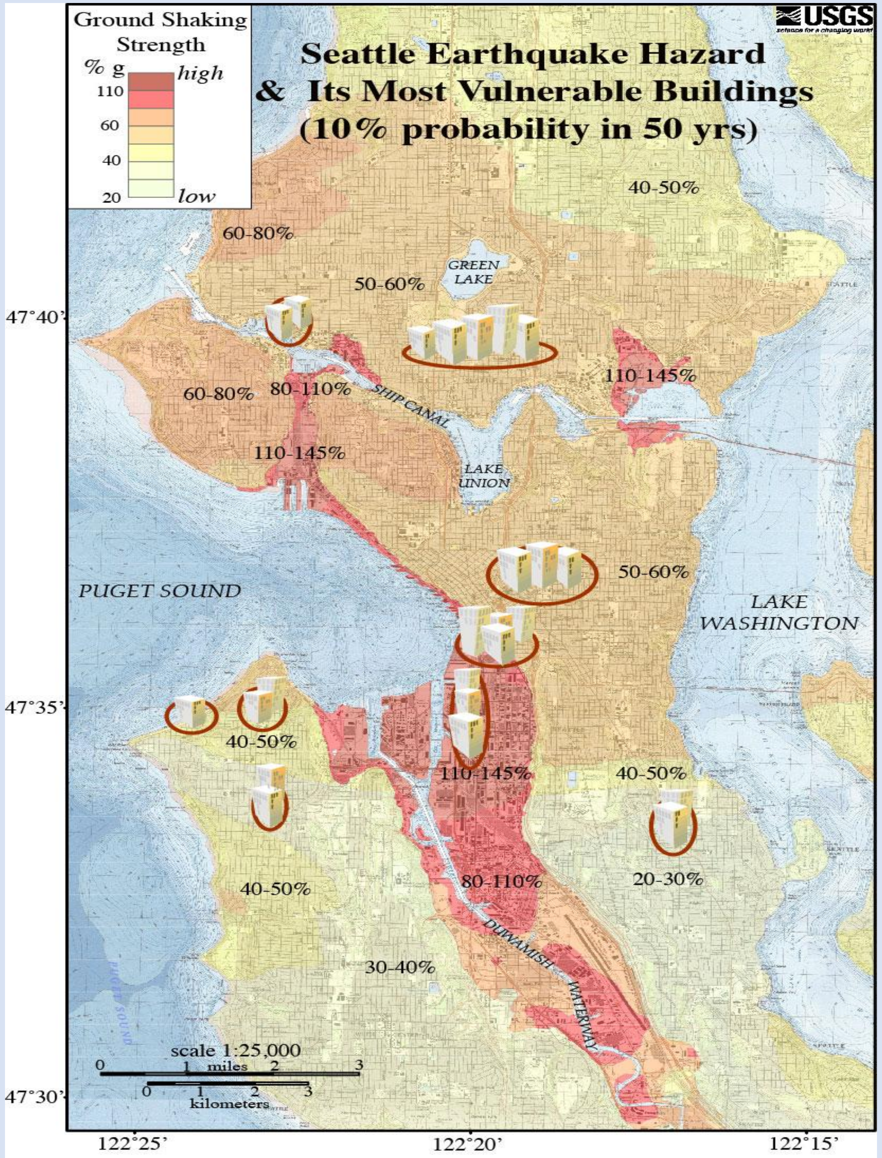

Once shaking stops, inspections begin and engineers and policy-makers applaud the success of design codes that prevented structures from collapse and reoccupation to proceed quickly. Design codes used for modern buildings based on realistic simulations of ground shaking from a great subduction zone earthquake proved accurate, saving lives and billions of dollars.

Science enhances predictive shaking models

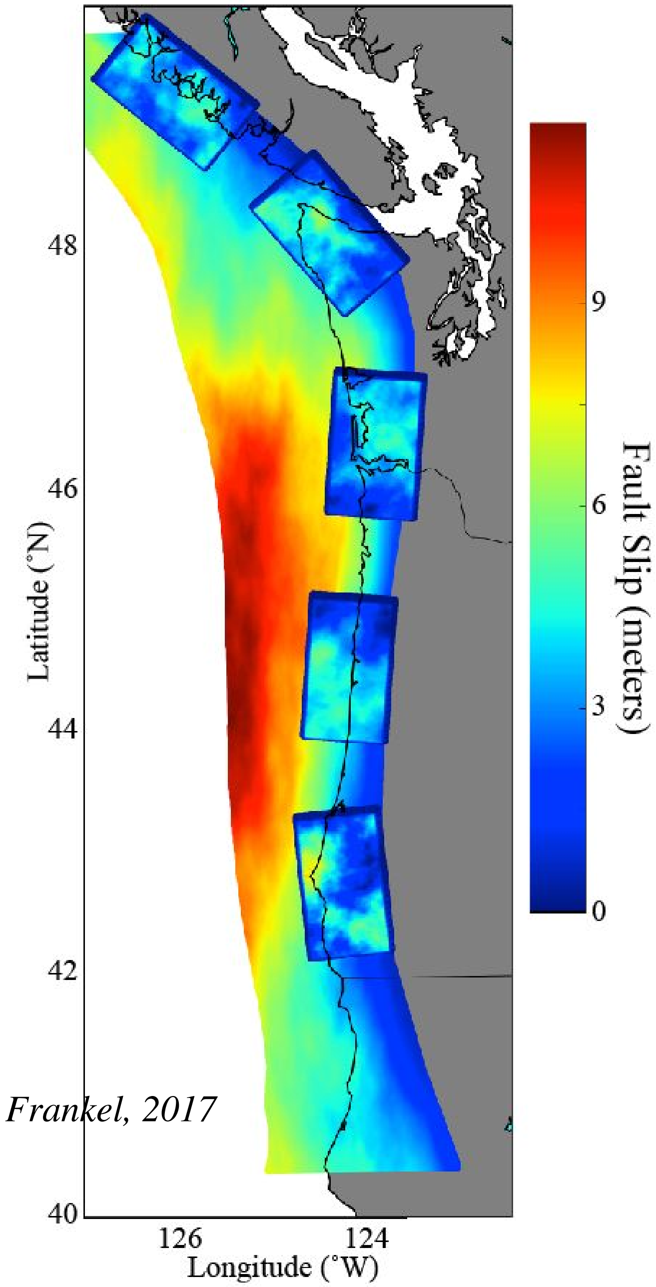

From Wirth & Frankel, 2017

smaller, more rapid slip on M8 patches radiates damaging high-frequencies

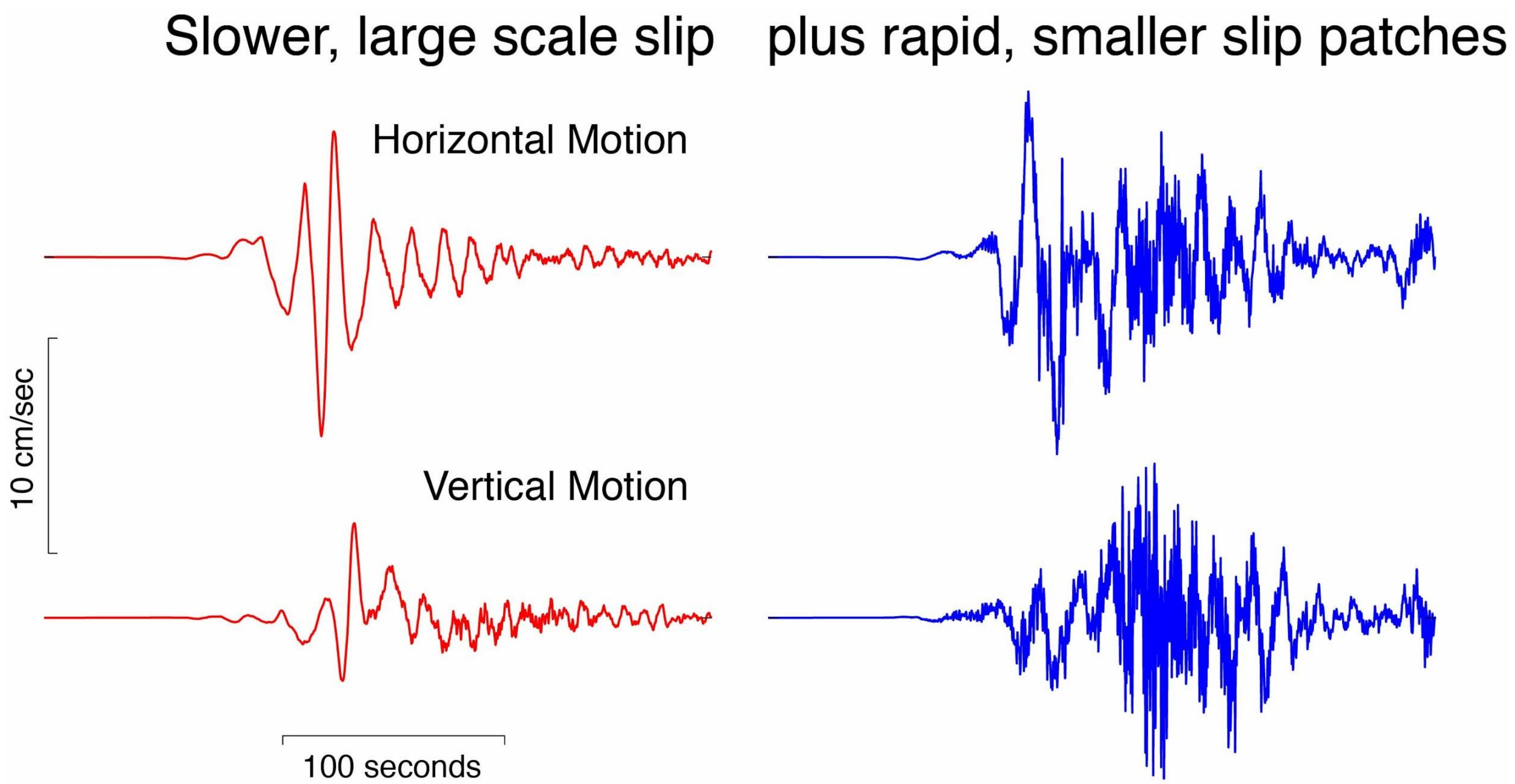

patchy slip/radiation verified observationally

Sub-event 1; Mw 8.5

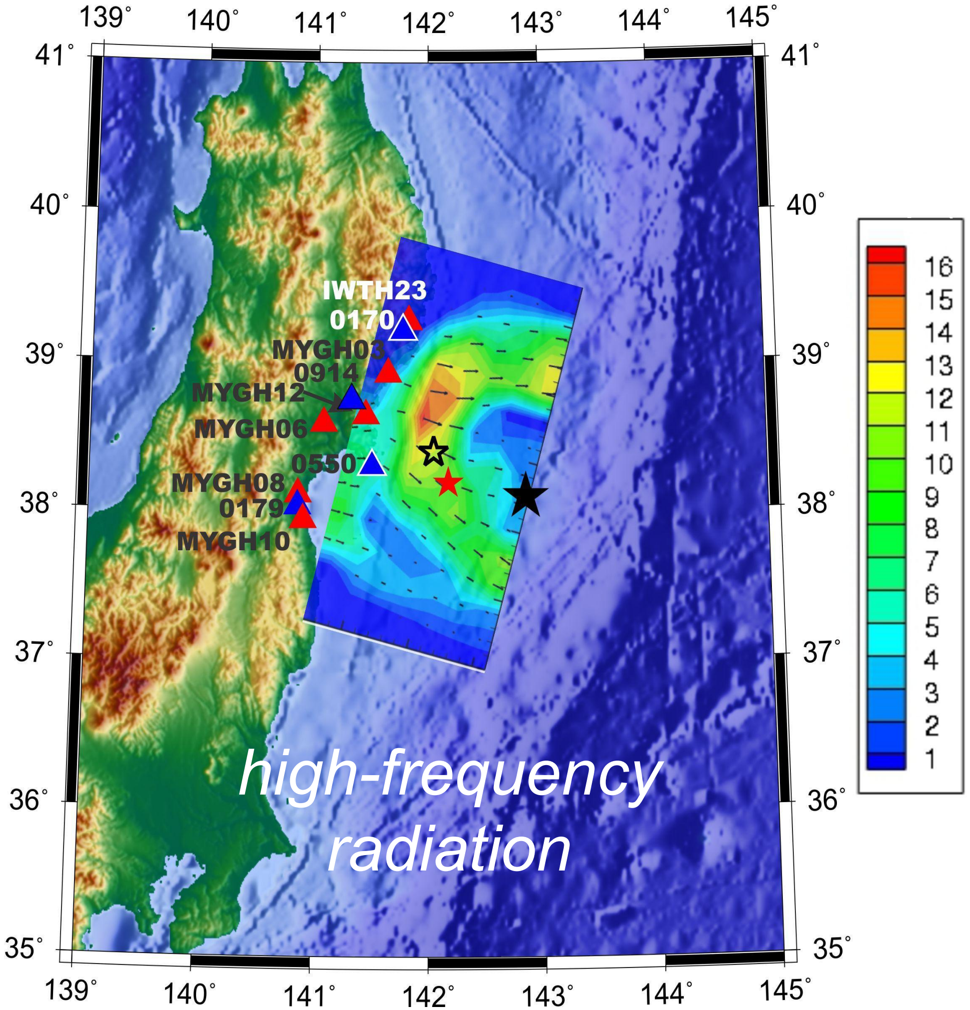

Sub-event 2; Mw 9.0, starts 35 s later

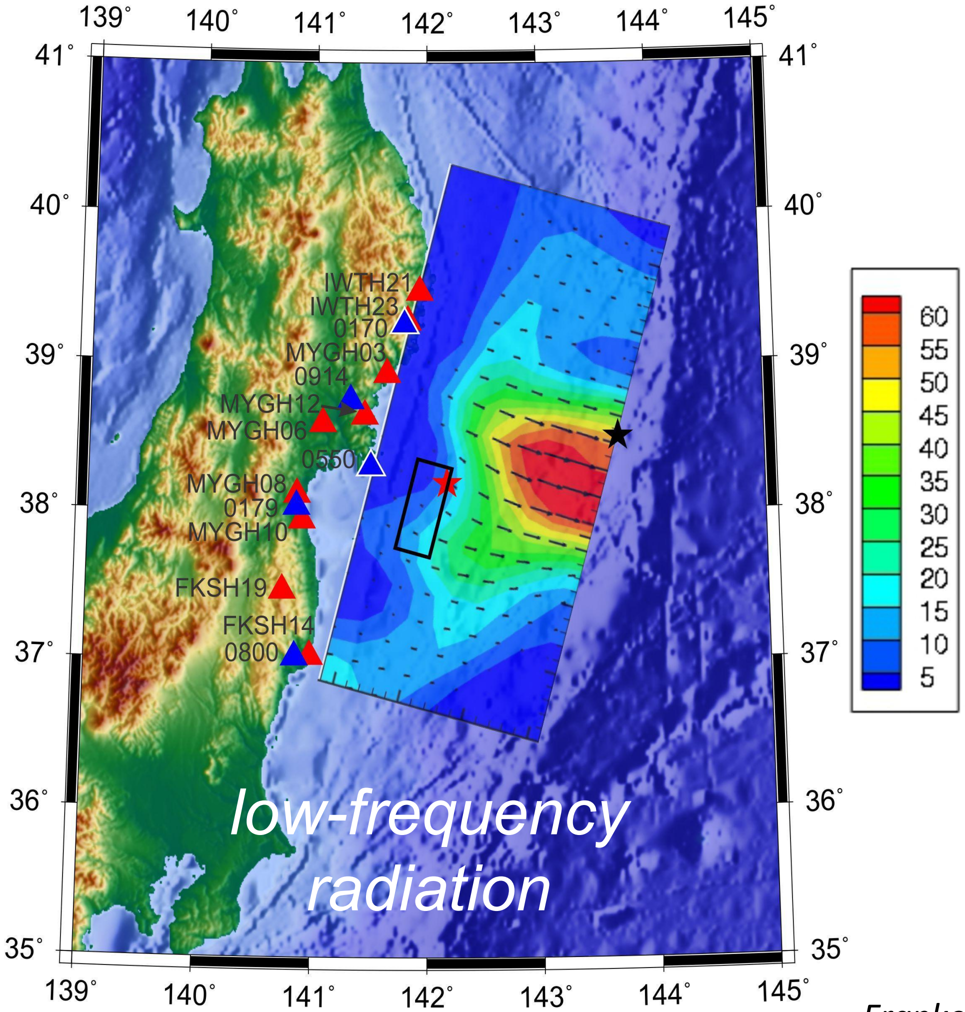

Frankel, 2017

slip compactness affects shaking durations, focusing

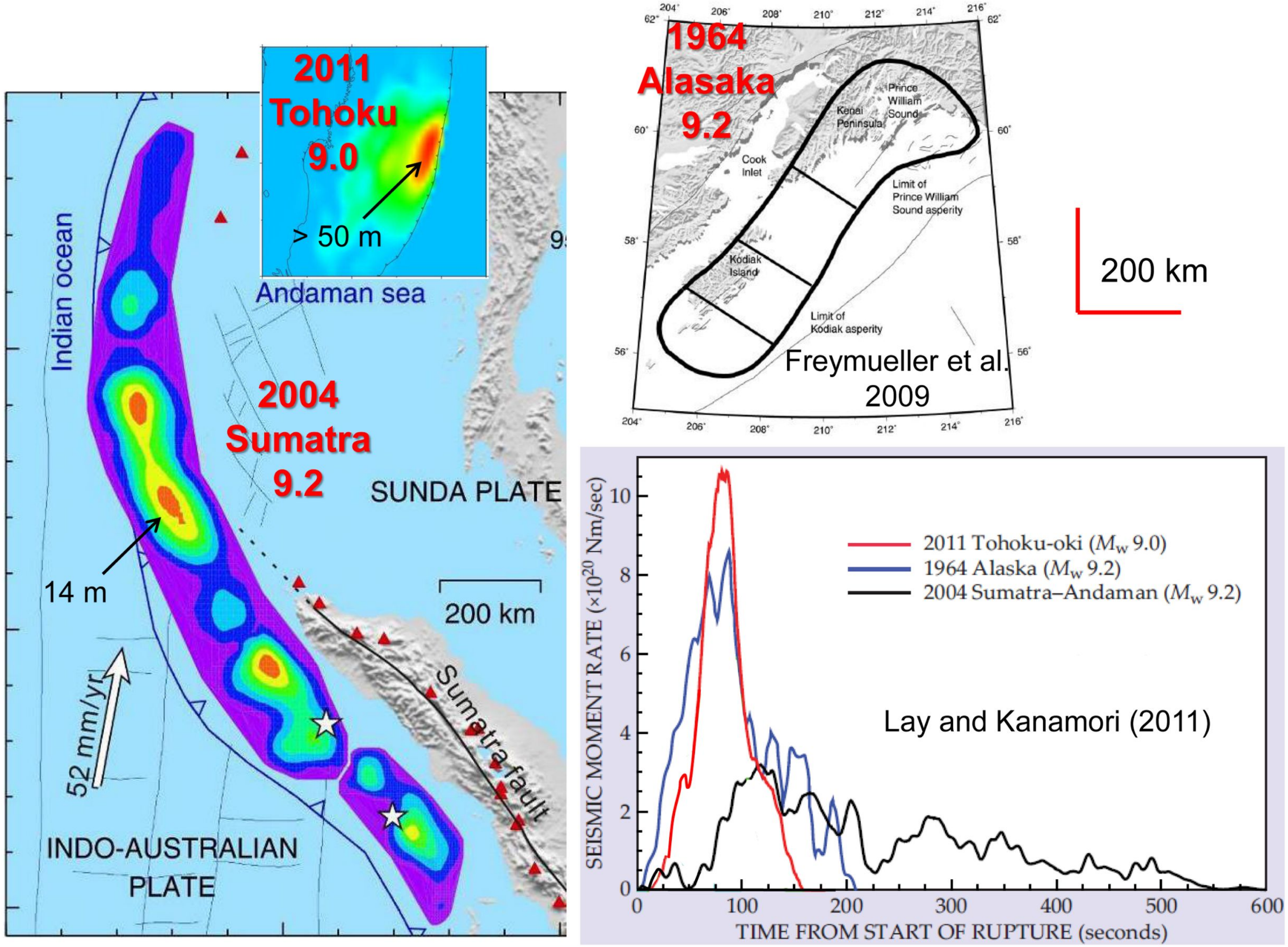

Wang, 2016

modeled shaking requires constraints from laboratory experiments

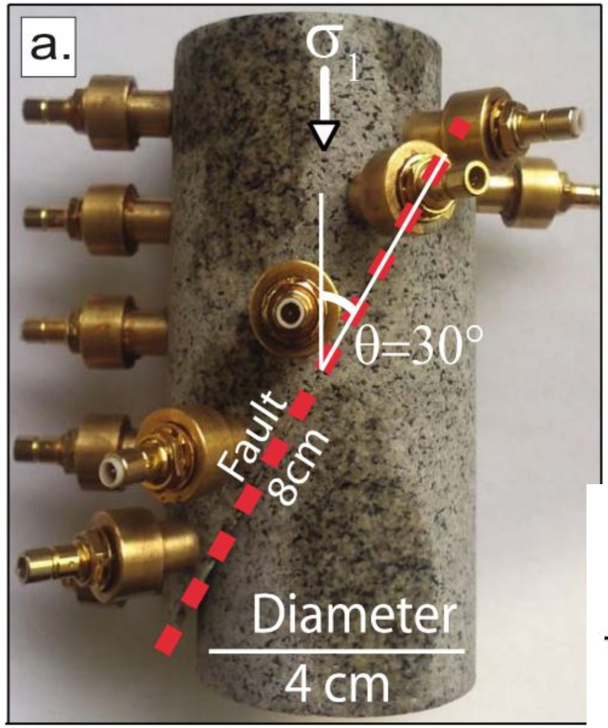

The only way to measure what's happening on the fault, during failure, & the dependencies on initial & environmental conditions.

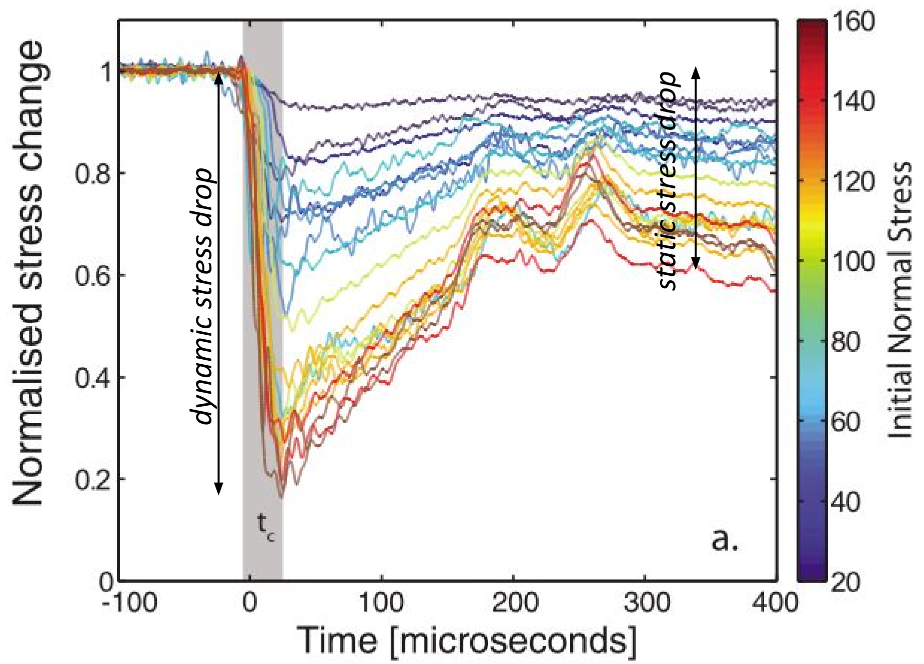

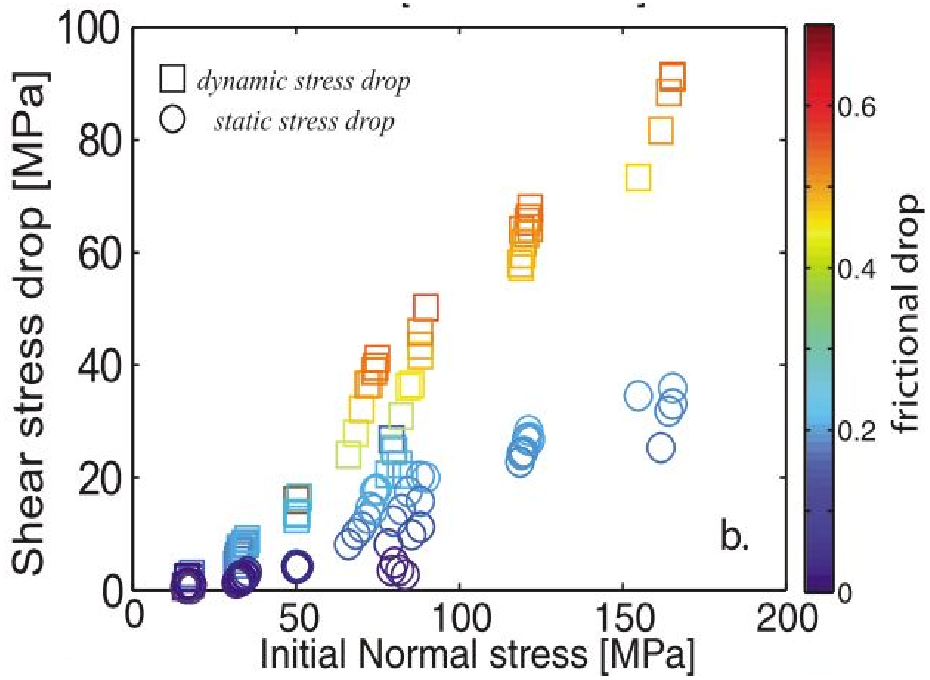

Dynamic rupture processes inferred from laboratory microearthquakes, *Passelègue, Schubnel, et al.*, 2016

Recovery proceeds,along with aftershocks

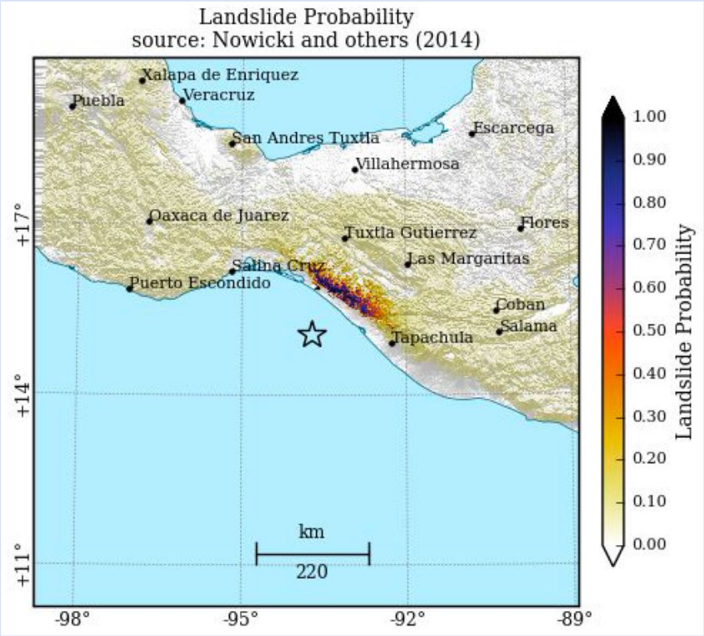

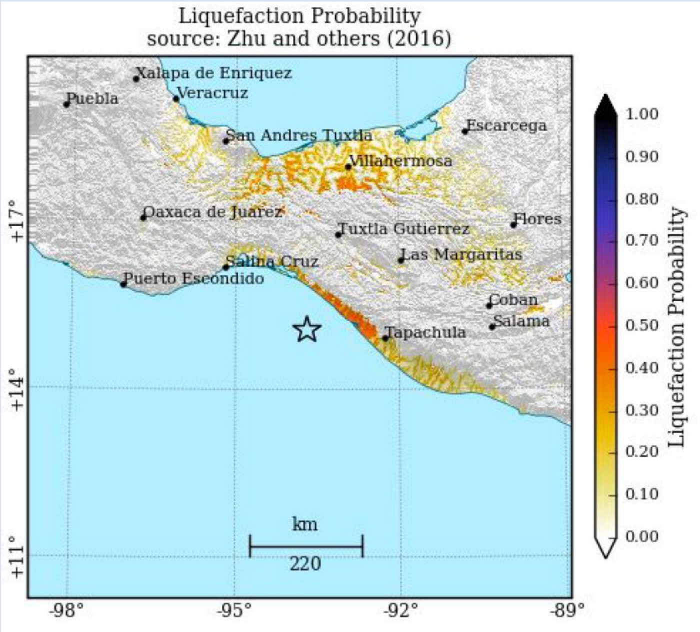

Just as residents begin taking stock of impacts, aftershocks cause the ground to tremble again and again. Their rates slow, but some exceed M7.5 and strike hundreds of km from the rupture zone. Multi-disciplinary monitoring networks issue updated forecasts regularly, foretelling not only of the changing rate, but also of where aftershocks are most likely to strike. These calm a nervous public and guide decisions about when and where engineers may safely inspect, and insurance companies and businesses may wisely rebuild.

Forecasts rely on understanding seismicity rate changes

temporally and spatially!

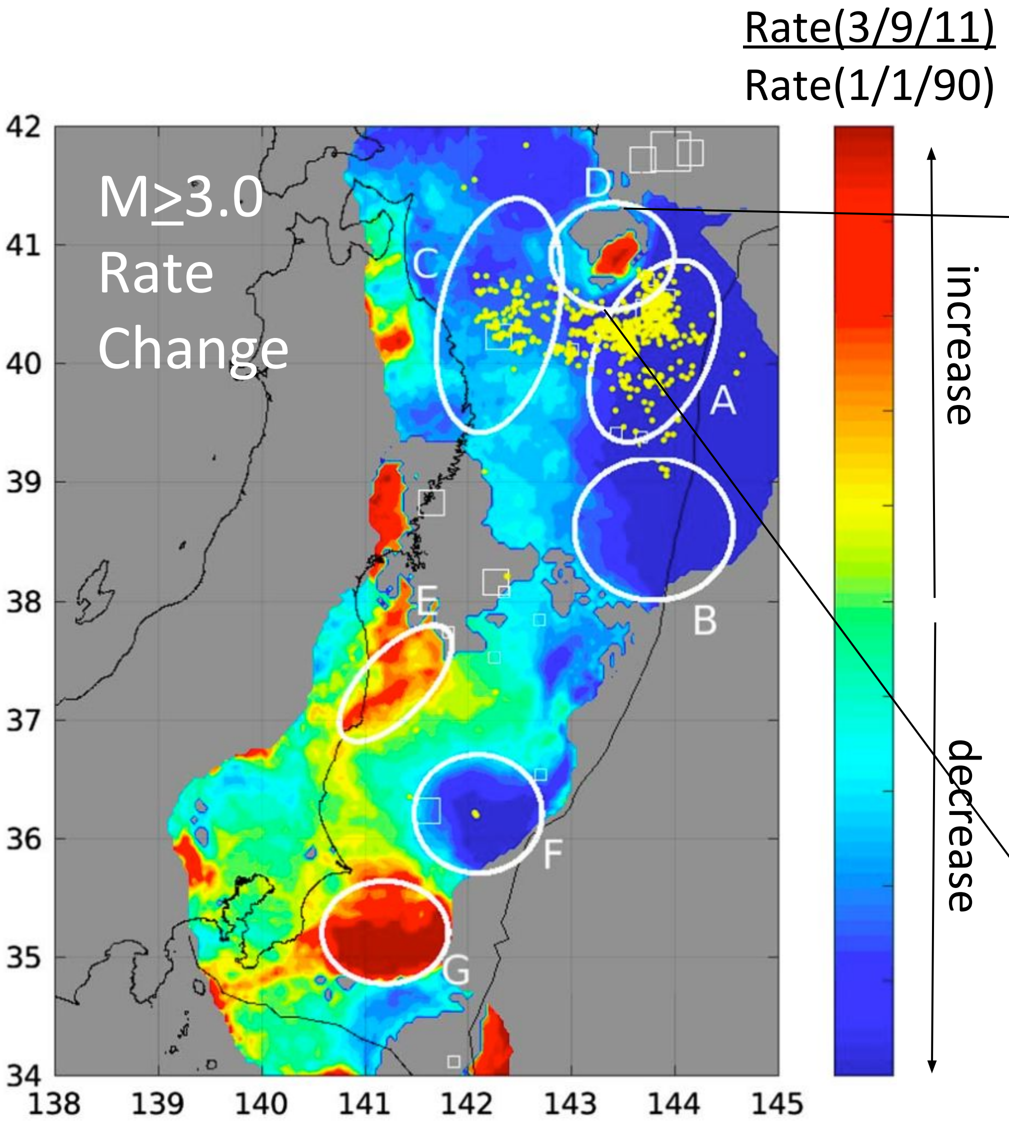

forecast aftershocks & quiescences?

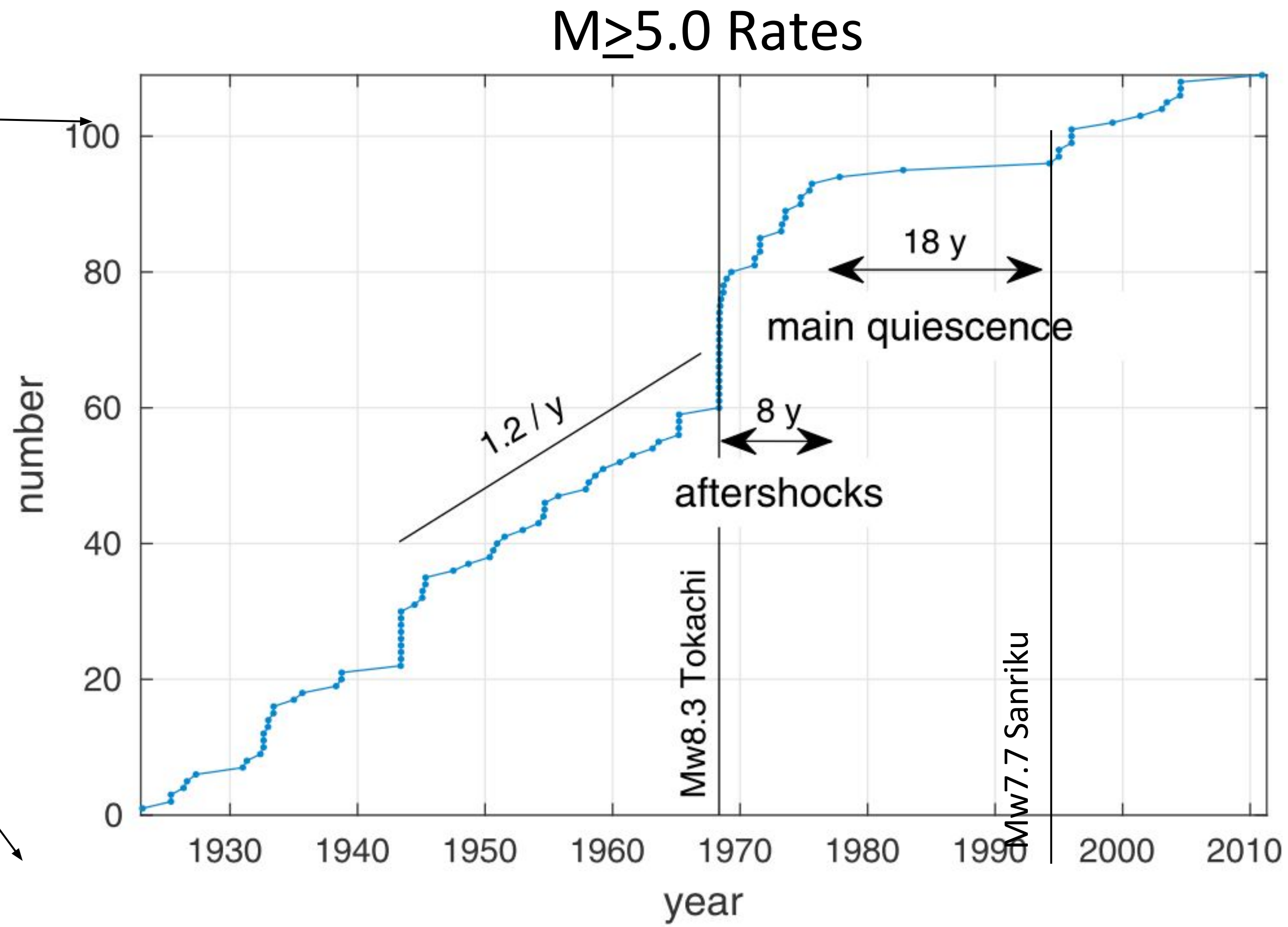

Change in seismicity along the Japan trench, 1990–2011, and its relationship with seismic coupling, Marsan et al., 2017

advances result from broad scientific perspectives

Ground-motion Fingerprinting

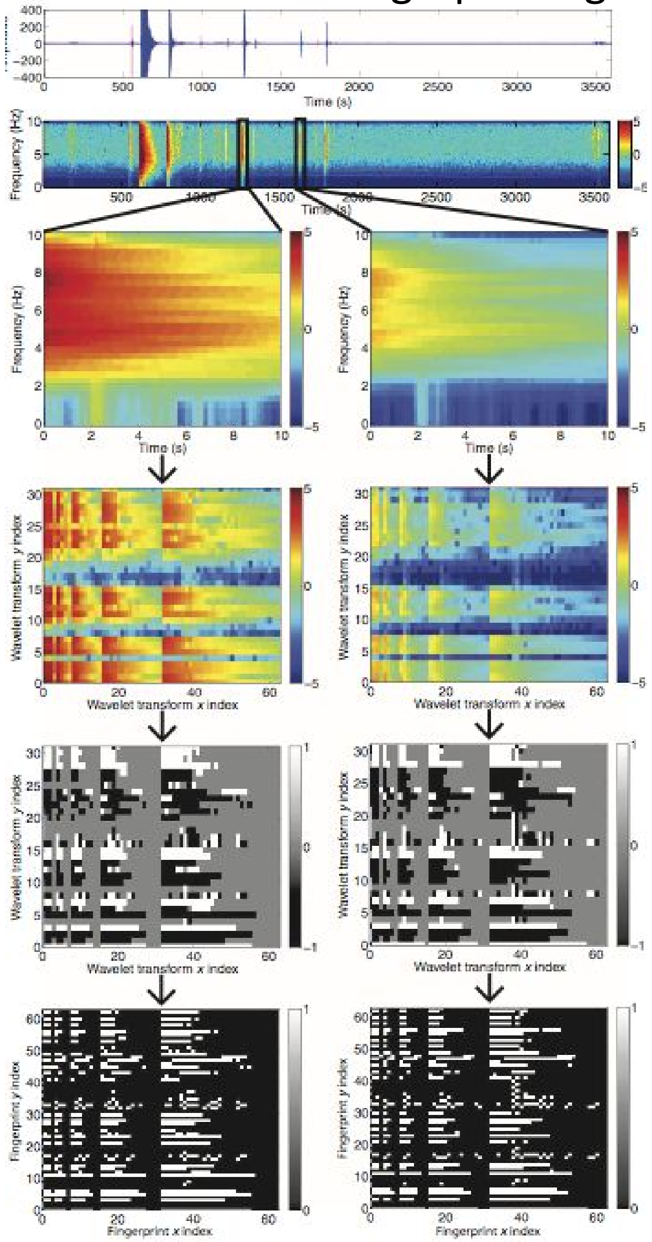

rapid, automated event detection

Earthquake detection through computationally efficient similarity search, *Yoon…Beroza*, 2015

advances result from broad scientific perspectives

Ground-motion Fingerprinting

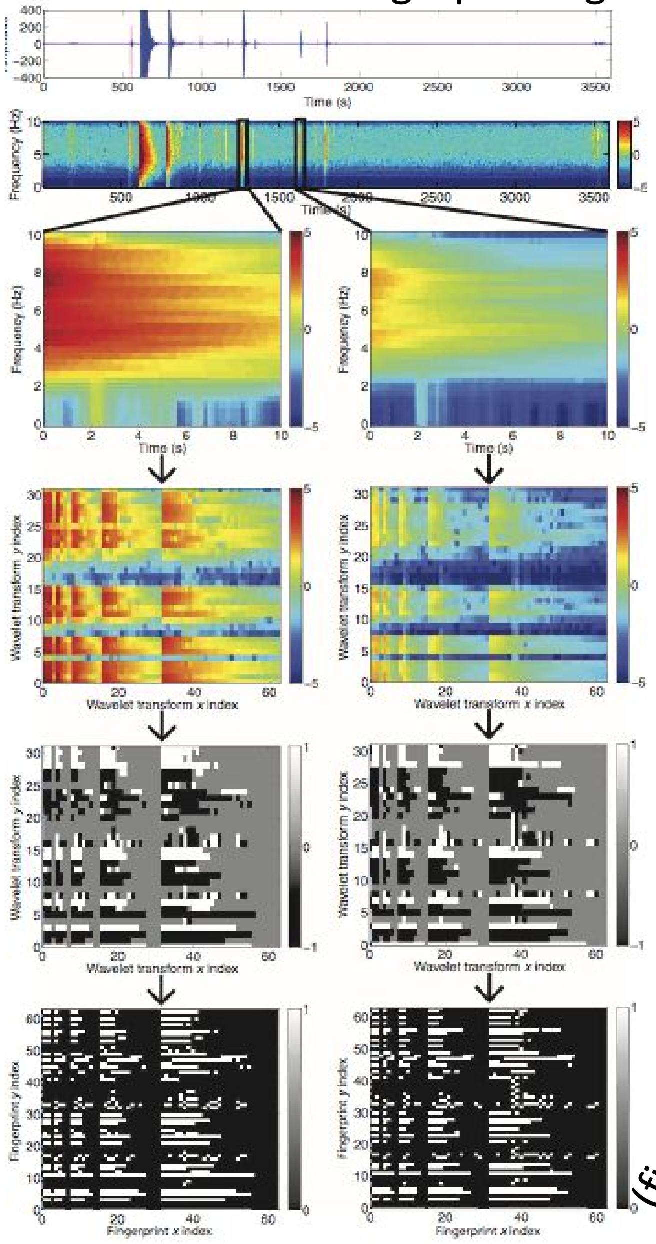

rapid, automated event detection

Fast sorting for similarity-based event detection.

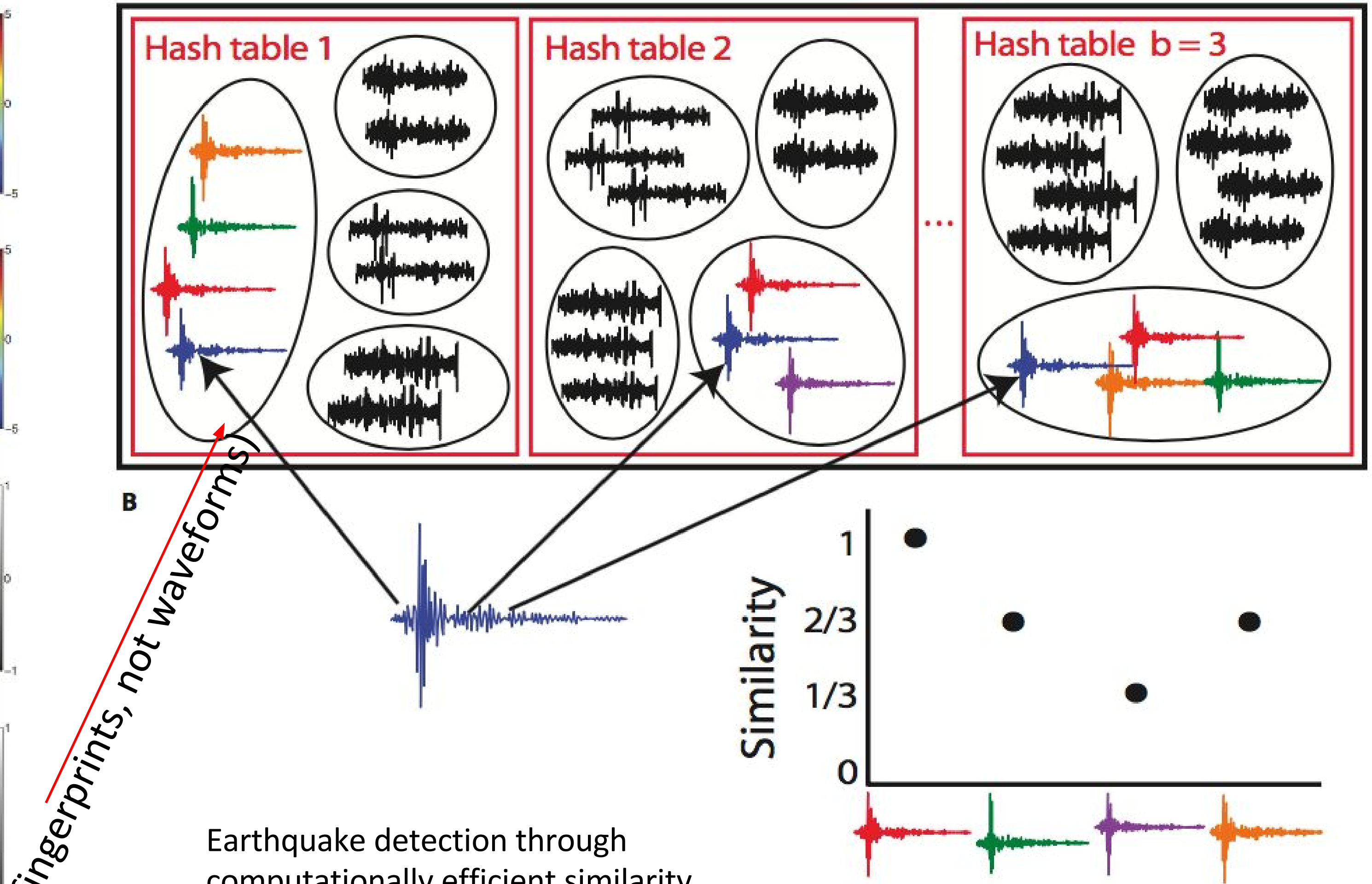

Earthquake detection through computationally efficient similarity search, *Yoon…Beroza*, 2015

Uniform California Earthquake Rupture Forecast (7-Days)

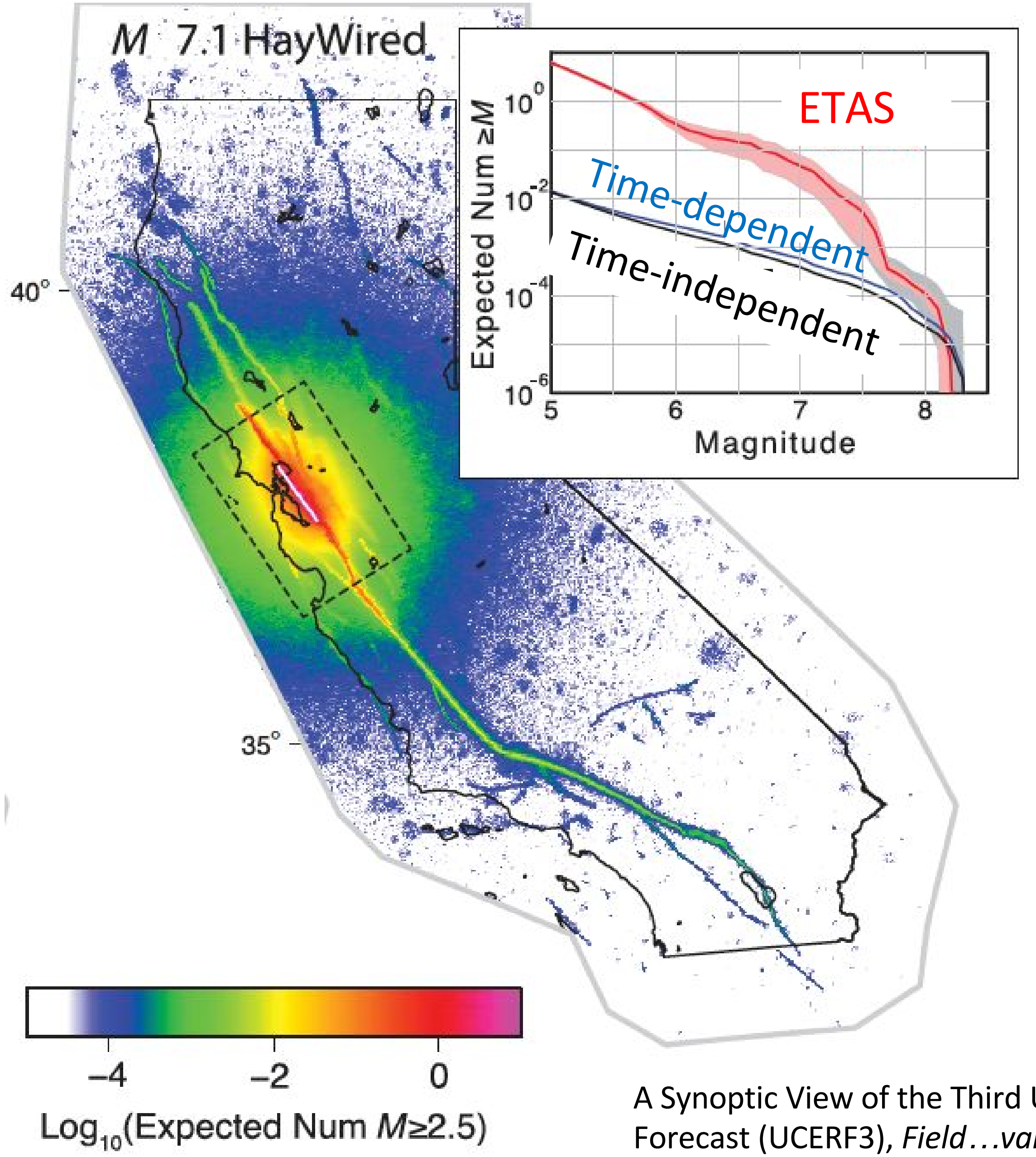

forecasts consistent over hours to millenia require coordinated science & model testing

A Synoptic View of the Third Uniform California Earthquake Rupture Forecast (UCERF3), *Field…van der Elst, et al.,* 2017

Anticipated ground failures do no harm.

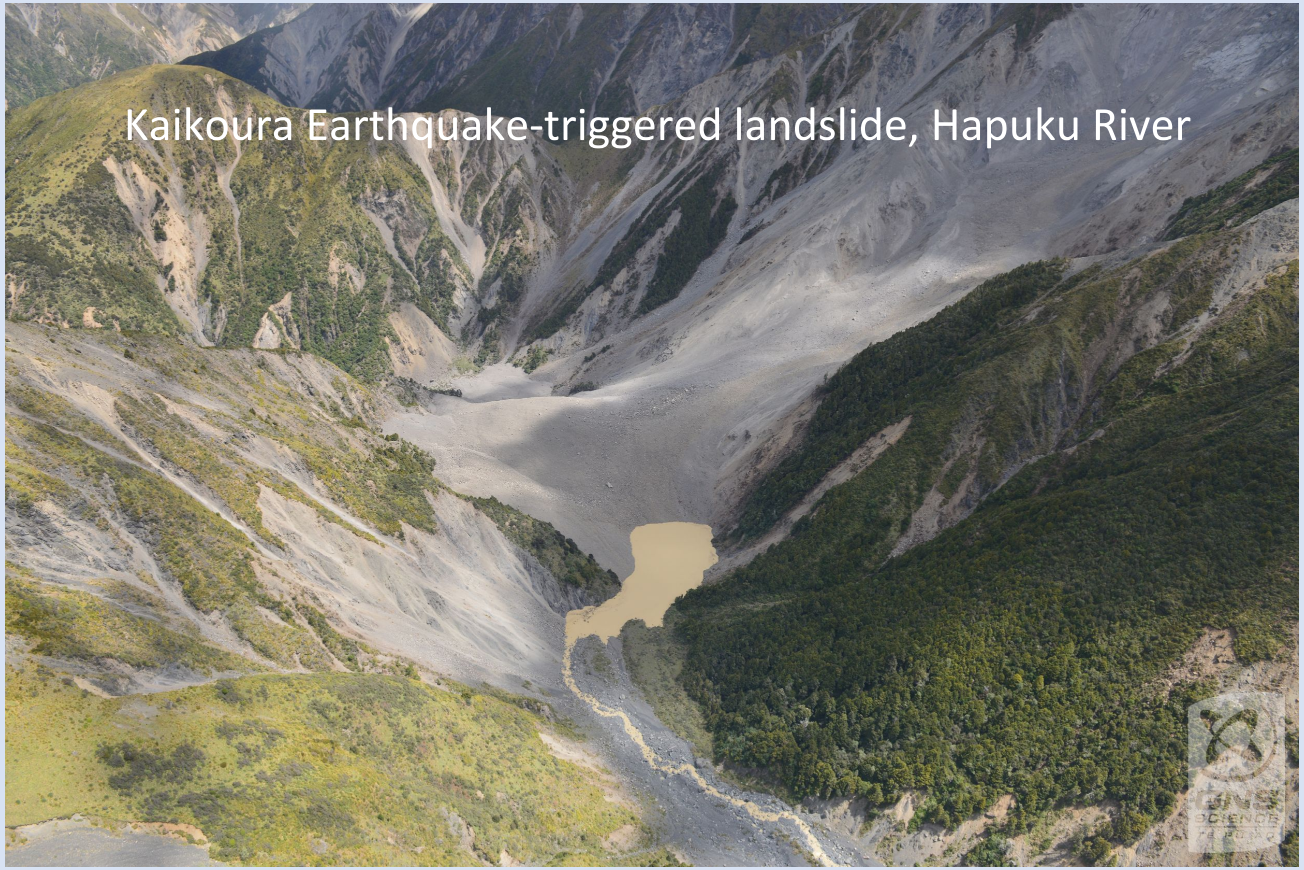

Repeated shaking and delayed failures causes steep slopes to fail and slide, and areas built atop fill and river sediments to liquefy, both onshore and offshore. An offshore landslide generates another localized tsunami, but was anticipated as unstable submarine slopes were obvious in coast-crossing hazard maps

High-resolution imagery & accurate failure/flow models may guide resilient zoning.

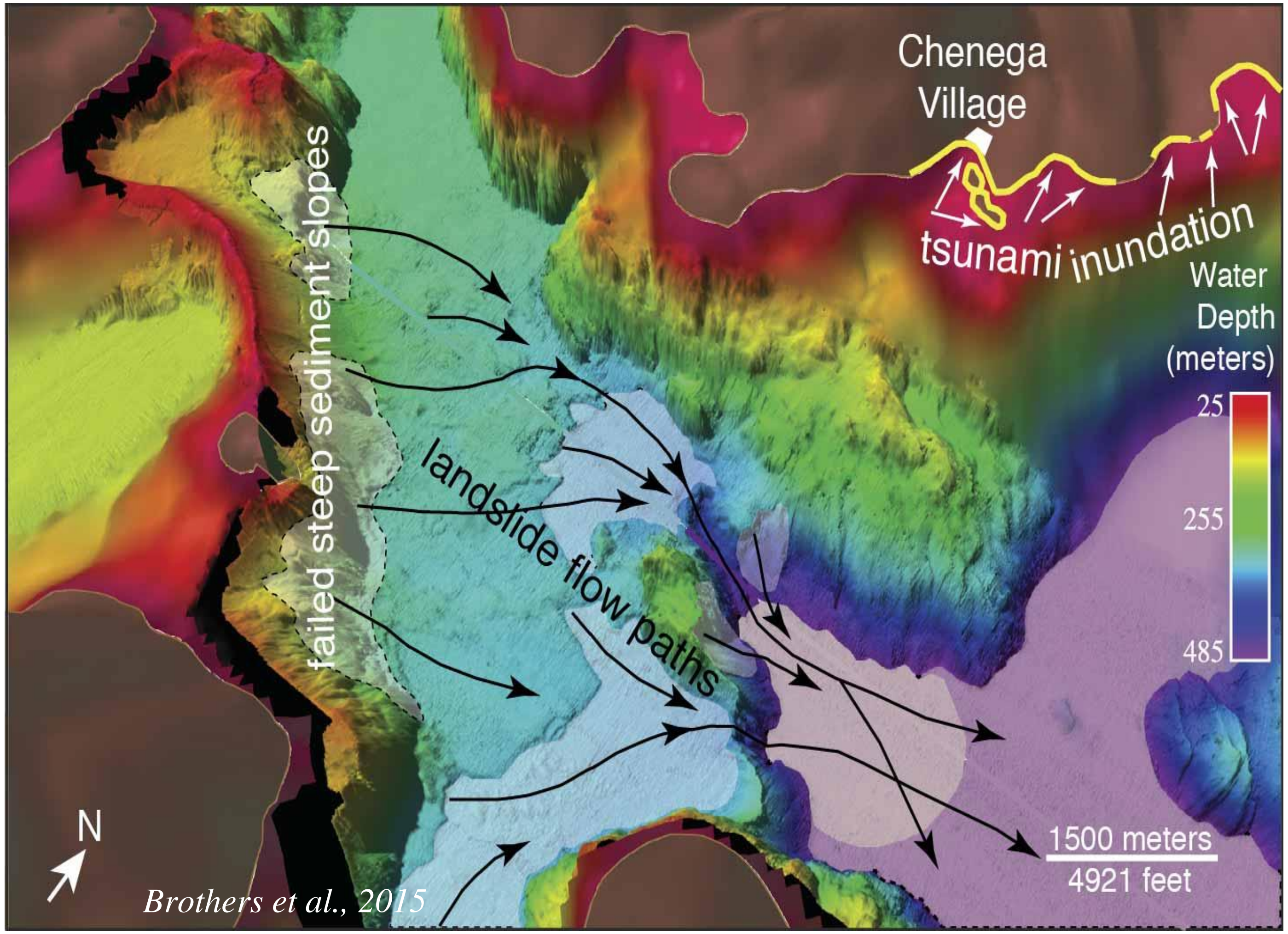

The 1964 M9.2 Alaska megathrust earthquake triggered an extraordinarily large and devastating tsunami at Chenega Village (23 fatalities). High-resolution seafloor topography revealed that the shaking caused a coastal landslide, which generated tsunami waves that were larger than those from the M9.2 earthquake.

Studies of analog slipping systems provide transferable insights to physics of slip.

Earthquakes

Loading: tectonic motion, creep

Where: fault surfaces

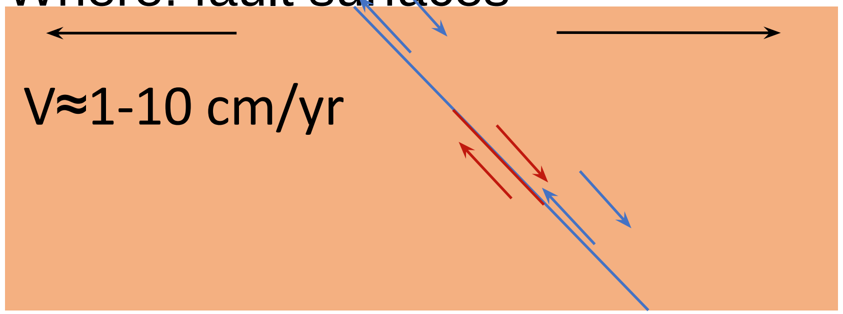

Sources: Asperities (geometric, lithologic irregularities)

Ice-quakes

Loading: gravity, glacial slip

Where: ice/bed interface

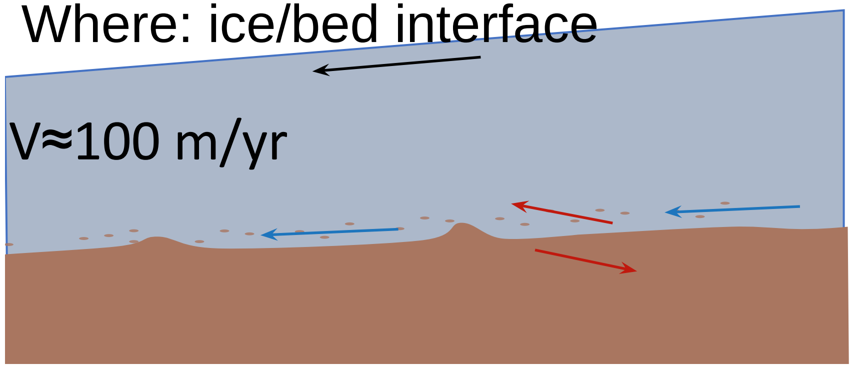

Landslide-quakes

Loading: gravity, rockslide movement

Where: sediment/basement interface

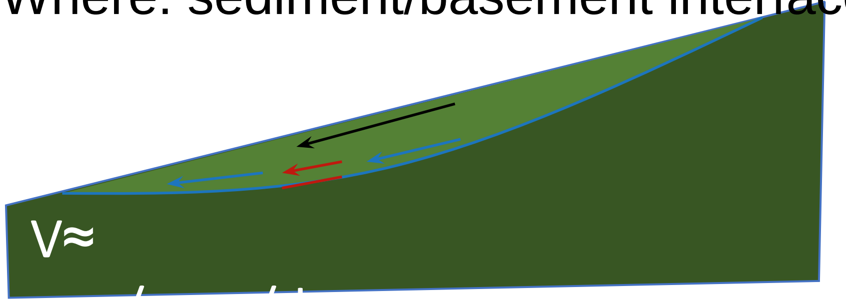

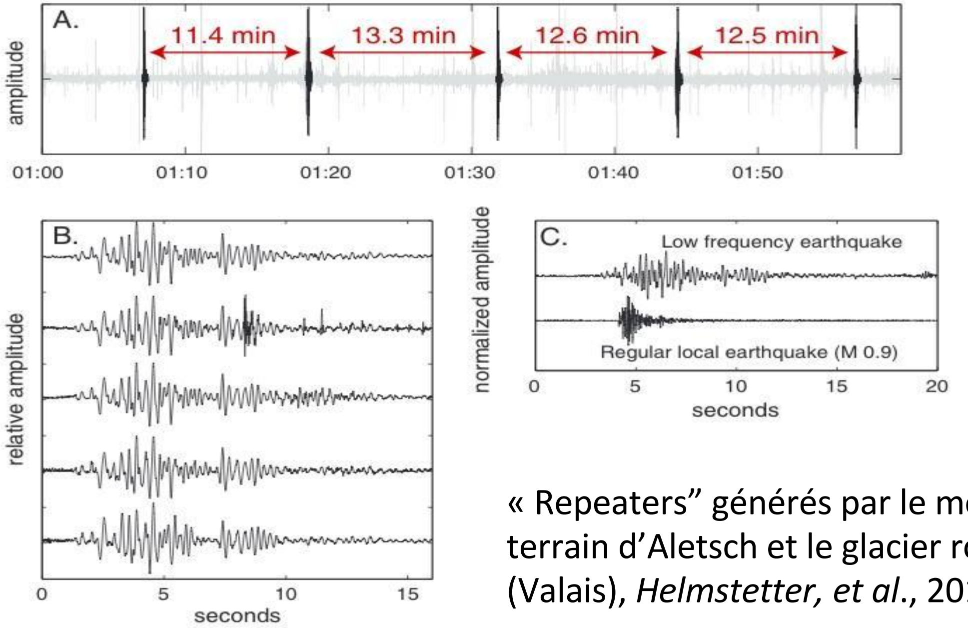

« Repeaters” générés par le mouvement de terrain d’Aletsch et le glacier rocheux de Gugla (Valais), *Helmstetter, et al.*, 2017

Shaking awakens volcanoes.

Rates of tiny earthquakes rise at one of the high-risk volcanoes, and glacial summit ice begins melting at another, culminating in an enormous river of mud and water that rushes down the mountain. The lahar warning system sends alarms to citizens living along the likely flow path, who evacuate. Ash cloud warnings guide airplanes to new courses that avoid catastrophic intersections. Quiescence at other volcanoes is confirmed and air traffic continues safely and without unnecessary shutdowns.

Science and monitoring underlie mitigation and warning.

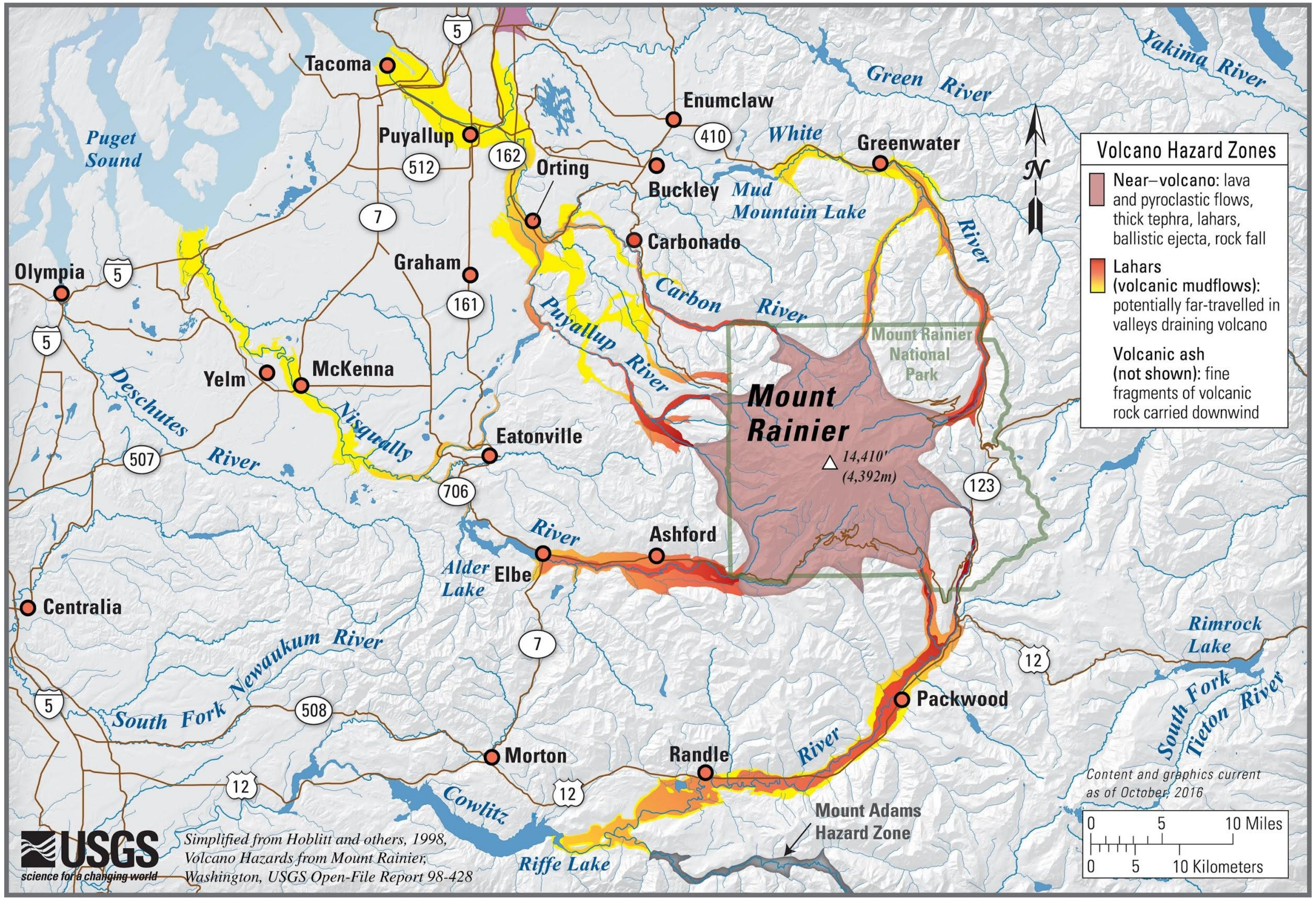

modeling & high-resolution data elucidate mechanics of cascading phenomena

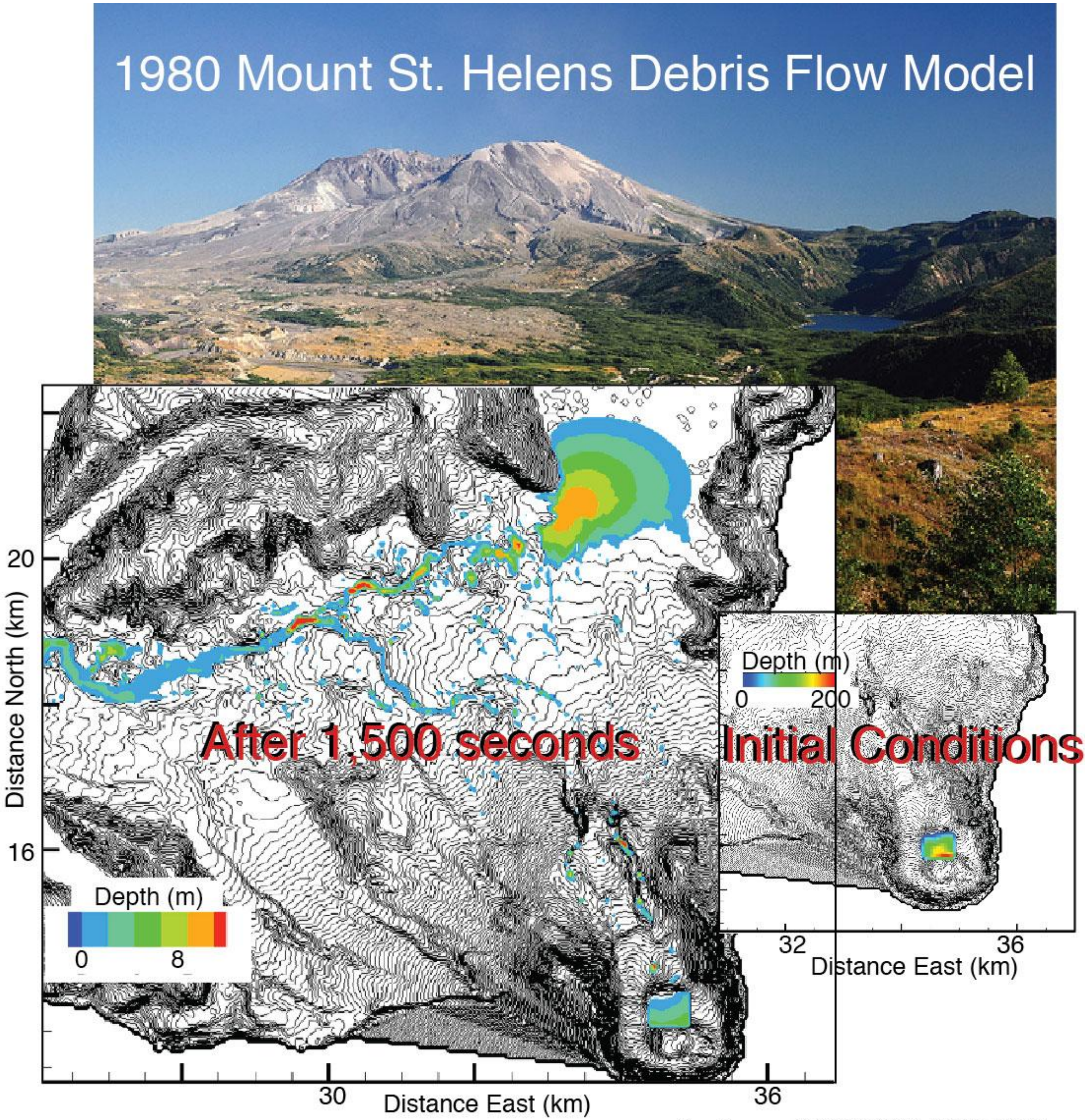

Denlinger, USGS OFR 2011-1317

On May 18th, 1980 a M5.1 earthquake caused the summit bulge to collapsed, uncorking a spectacular eruption. Shaking broke a natural dam, releasing massive debris flows. LiDAR data validate numerical modeling, to be used for future forecasting.

A prosperous, happy inter-seismic period.

It's the year <u>2026</u> in northwest Washington state, USA. Recovery from last year's powerful events is complete and life goes happily on!

USGS
science for a changing world